1. Report No.	2. Government Accession No.	3. Recipient's Catalog No.
TX-96/2919-1		

4. Title and Subtitle	5. Report Date
Evaluation of Stabilized Base Durability Using a Modified South African Wheel Tracking Device	October 1995
	6. Performing Organization Code
7. Author(s)	8. Performing Organization Report No.
Petrus Gerhardus Van Blerk and Tom Scullion	Research Report 2919-1
9. Performing Organization Name and Address	10. Work Unit No. (TRAIS)
Texas Transportation Institute The Texas A&M University System College Station, Texas 77843-3135	11. Contract or Grant No. Study No. 7-2919
12. Sponsoring Agency Name and Address	13. Type of Report and Period Covered
Texas Department of Transportation Research and Technology Transfer Office P. O. Box 5080 Austin, Texas 78763-5080	Interim: Sept. 1994-Sept. 1995
	14. Sponsoring Agency Code

15. Supplementary Notes

Research performed in cooperation with the Texas Department of Transportation.
Research Study Title: Spall Repair, Base and Subgrade Stabilization, and Non Destructive Test (NDT) Service for the Houston District, Phase II.

16. Abstract

This study was initiated to investigate the durability of the cement treated base (CTB) material used extensively by the Houston District. A literature review concluded that the most realistic durability test is the Rolling Wheel Tracker developed by the South Africans. Typical Houston CTBs were tested with this wheel tracker, and the testing procedure was modified so that both linear shrinkage and unconfined compressive strength could also be measured on the same test specimen.

Testing included field samples from SH 36 near Rosenburg, Texas, which had exhibited extensive deterioration after only a few years in service. Tests were also performed at 3 stabilizer contents, on laboratory molded samples of two aggregates. The first was a high quality limestone material with very low PI < 2. The second was a poor material with clay contaminated fines PI = 7.4 (still within TxDOT specifications).

From this study it was concluded that:

a. lack of Abrasion Resistance was not the principal cause of the failure of SH 36 (See Companion Report 2919-2 on Chemical Deterioration);
b. with good aggregates the lower stabilizer content (4%) produced a material which was capable of meeting TxDOT strength requirements and also had acceptable shrinkage and durability characteristics; and
c. the CTB containing high PI fines exhibited high shrinkage. It is anticipated that this material would crack extensively in the field.

The modified South African Wheel Tracking Device shows good potential for determining performance related material characteristics which can be used to establish the optimum stabilizer content for any possible base material.

17. Key Words	18. Distribution Statement
Cement Treated Base, Durability, Shrinkage, Wheel-Tracking, and Design	No Restrictions. This document is available to the public through NTIS: National Technical Information Service 5285 Port Royal Road Springfield, Virginia 22161

19. Security Classif.(of this report)	20. Security Classif.(of this page)	21. No. of Pages	22. Price
Unclassified	Unclassified	88	

EVALUATION OF STABILIZED BASE DURABILITY USING A MODIFIED SOUTH AFRICAN WHEEL TRACKING DEVICE

by

Petrus Gerhardus Van Blerk
Graduate Assistant Research
Texas Transportation Institute

and

Tom Scullion
Associate Research Engineer
Texas Transportation Institute

Research Report 2919-1
Research Study Number 7-2919
Research Study Title: Spall Repair, Base and Subgrade Stabilization, and Non Destructive Test (NDT) Service for the Houston District, Phase II

Sponsored by the
Texas Department of Transportation

October 1995

TEXAS TRANSPORTATION INSTITUTE
The Texas A&M University System
College Station, Texas 77843-3135

IMPLEMENTATION STATEMENT

A wide variety of materials are used around the state of Texas in stabilized base layers. Mix design is usually based solely on compressive strength requirements where the engineer is recommended an allowable cement content of 4-9%. The Houston District is a large user of cement treated base (CTB) and cement contents of 5 - 6% are typical.

However, in a recently completed statewide evaluation of CTB performance several problem areas were identified. Initial strength was not the controlling factor in long term performance; in fact, above a certain stabilizer content there appeared to be an inverse relationship between strength and field performance. Shrinkage cracking and subsequent durability problems were often the issues controlling performance.

In this report a Modified Wheel Tracking device is introduced. Using this test procedure it is possible to measure three performance related characteristics of stabilized bases, namely compressive strength, linear shrinkage, and durability. Establishing criteria for all three should result in better performing materials and minimize problems caused by over stabilization of marginal materials.

DISCLAIMER

The contents of this report reflect the views of the authors, who are responsible for the facts and the accuracy of the data presented herein. The contents do not necessarily reflect the official views or the policies of the Texas Department of Transportation (TxDOT). This report does not constitute a standard, specification or regulation. It is not intended for construction, bidding or permit purposes. The engineer in charge of the project is Tom Scullion, P.E. #62683.

ACKNOWLEDGMENT

Pat Henry, P.E. of the Houston District, was Project Director on this study; his support and encouragement is greatly appreciated.

TABLE OF CONTENTS

LIST OF FIGURES

LIST OF TABLES

SUMMARY

This study was initiated to investigate the durability of the cement treated base (CTB) material used extensively by the Houston District. A literature review concluded that the most realistic durability test is the Rolling Wheel Tracker developed by the South Africans. Typical Houston CTBs were tested with this wheel tracker, and the testing procedure was modified so that both linear shrinkage and unconfined compressive strength could also be measured on the same test specimen.

Testing included field samples from SH 36 near Rosenburg, Texas, which had exhibited extensive deterioration after only a few years in service. Tests were also performed at three stabilizer contents, on laboratory molded samples of two aggregates. The first was a high quality limestone material with very low PI < 2. The second was a poor material with clay contaminated fines PI = 7.4 (still within TxDOT specifications).

From this study it was concluded that:

a. lack of Abrasion Resistance was not the principal cause of the failure of SH 36 (See Companion Report 2919-2 on Chemical Deterioration);
b. with good aggregates the lower stabilizer content (4 percent) produced a material which was capable of meeting TxDOT strength requirements and also had acceptable shrinkage and durability characteristics; and
c. the CTB containing high PI fines exhibited high shrinkage. It is anticipated that this material would crack extensively in the field.

The modified South African Wheel Tracking Device shows good potential for determining performance related material characteristics which can be used to establish the optimum stabilizer content for any possible base material.

CHAPTER I: BACKGROUND AND INTRODUCTION

BACKGROUND

During the last few years the Texas Department of Transportation (TxDOT) experienced two major failures of cement treated bases (CTBs) in the Houston district. The first occurred on a widening project on US 290 near Hempstead, Texas, where the CTB disintegrated shortly after construction. Examination of cores taken from the pavement indicated that the cement had washed out from the base, resulting in a virtually unstabilized material. This section was removed and replaced with an asphalt stabilized base. The second failure occurred near Orchard, Texas, on State Highway 36. In this case the new CTB disintegrated around transverse cracks in the wheel paths.

Transverse and block cracking occurred shortly after construction. It appeared that water was trapped within the stabilized layers of the pavement, which may have led to accelerated disintegration. Examination of cores taken from the distressed areas showed clean, large aggregates, with the fine material apparently pumped out, Figure 1.1 shows this. Cores taken in the undistressed areas were intact and showed no sign of fines loss. However, closer examination of insitu samples taken from the undistressed shoulder of the road showed the bottom half of the stabilized layer had deteriorated more rapidly than the top half, Figure 1.2 illustrates this.

It was initially thought that the failure on SH 36 was because of mechanical deterioration. The following phases were proposed to describe the deterioration mechanism.

•Phase 1: Shrinkage and thermal cracking developed shortly after construction because of the cement stabilization. These cracks developed in the cement treated base but propagated through the Hot Mix Asphaltic Concrete (HMAC), thus allowing water to penetrate the base layer. However, the base consisted of a crushed limestone material treated with 6 percent cement, and the subbase consisted of pulverized original pavement material treated with 6% cement. The pavement structure of SH 36 is shown in Figure 1.3. Because of the measured different thermal properties of the cement treated layers, the cracks that developed in each layer were at different intervals, which resulted in water being trapped between the treated layers.

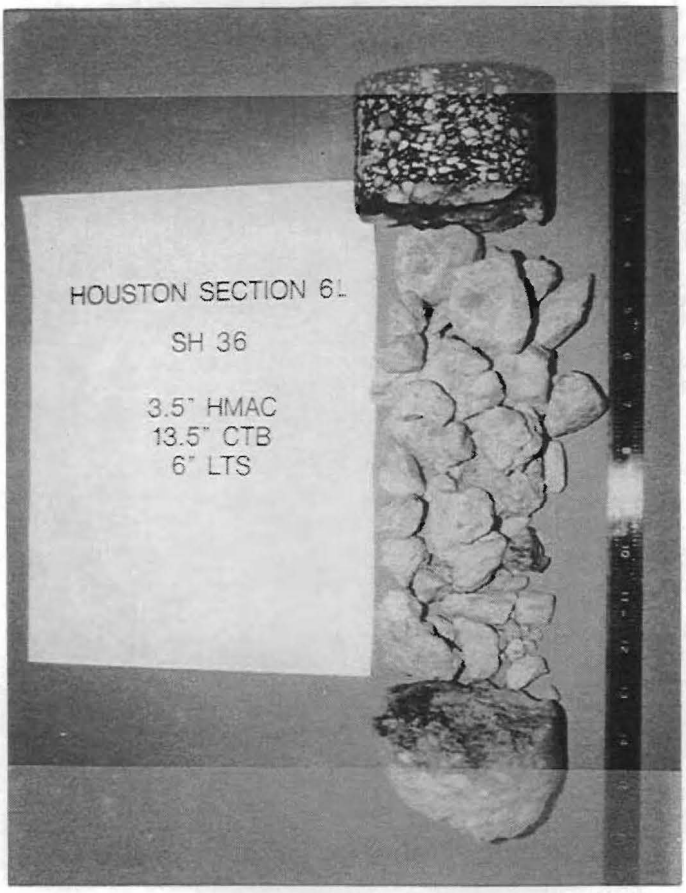

Figure 1.1. Disintegrated Cement Treated Base Layer Showing Clean, Large Aggregates with the Fine Material Apparently Pumped Out.

Figure 1.2. In situ Sample from SH 36 Shows the Bottom Half of the Cement Treated Base Deteriorated More Rapidly than the Top Half.

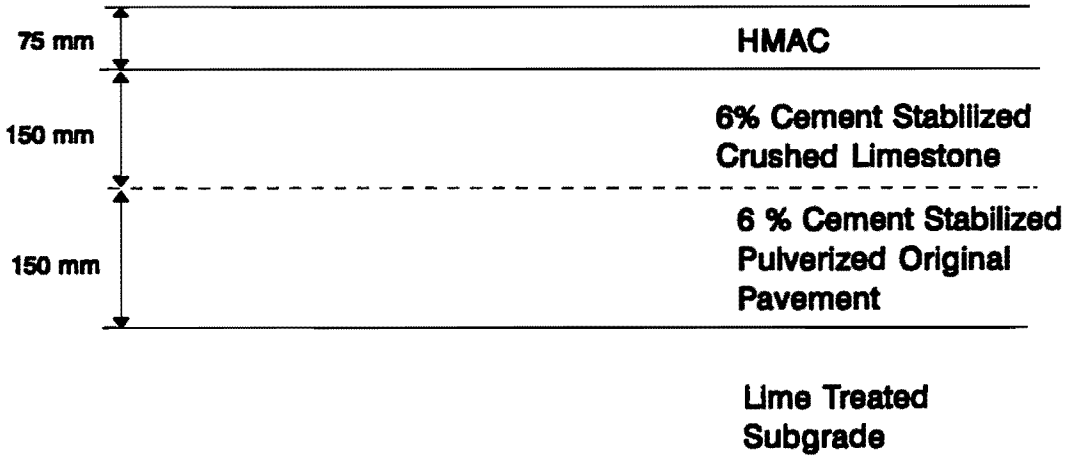

Figure 1.3. Pavement Structure of SH 36.

•Phase 2: Under wet conditions, moisture penetrated the base layer through cracks in the HMAC. However, this moisture was trapped between the base and subbase layers, and under the action of traffic high water pressures could develop. This would then lead to pumping of the fines under the repeated action of the traffic.

•Phase 3: Finally, under increasing traffic action the fines would be pumped out and the mechanical abrasion and erosion action that developed between the HMAC layer and the base layer would help to deteriorate the base layer. This would then leave the clean larger aggregates with no binder material, and as a result failure of the base layer occurred.

It was therefore decided to test this failure hypothesis by performing different laboratory tests to determine the durability of the CTB. Strength tests performed on the solid cores yielded Unconfined Compressive Strength (UCS) values in excess of 6900 kPa, which is well in excess of the specified UCS of 4140 kPa. It appears that the main reason for the distress development may have been trapped moisture. However, the rate of the distress development, as well as the severity, indicates that there may also be a durability problem with the CTB material used. The purpose of this report is to investigate the factors that influence the durability of cement treated materials. In addition, this study is also aimed at exploring different methods of durability testing for cement treated materials.

CHAPTER II: LITERATURE SURVEY

INTRODUCTION

Stabilization of pavement materials is not a new concept in pavement construction. However, stabilization of natural materials is a complex science which, if not properly understood, may lead to premature pavement failure. Materials that are mainly used for stabilization of pavements include cement, lime, fly ash, and asphalt. Stabilization is often performed because of the gradual depletion of good paving materials. Consequently, engineers are continually forced to make use of substandard material in pavement construction. In the Houston district unstabilized flexible bases have not performed well on their poor subgrades, and high ground water tables, this led to the use of stabilized bases 10 to 15 years ago. This, together with ever increasing traffic volumes have prompted the need for stronger and more durable pavement materials. Also the construction of high performance pavements on poor subgrades and the increased construction of super highways led to the design of pavements with higher strength and durability, which can be attained by using stabilization.

FACTORS INFLUENCING FAILURE OF A CEMENT TREATED BASE

The development of the properties of cement treated materials is further complicated by variations in the cement content, curing time, curing conditions, and the deleterious effects of past loadings and weathering. The UCS test is most commonly used to predict the suitability of a soil-cement mixture for structural or modification applications. Generally, the strength of a soil-cement mixture increases with increasing density (10). Also water content at a specific compaction effort and the compaction method may also affect the strength of the soil-cement mixture. The following pages discuss the factors that can lead to premature failure of a cement-soil mixture.

Volume Change and Shrinkage

The amount of shrinkage that cement stabilized materials exhibit during curing and drying depends on the cement content, aggregate type (particularly the fine aggregates),

water content, degree of compaction, and curing conditions (5, 6). Cement treated pavements generally exhibit a fairly extensive pattern of transverse cracking soon after construction. This type of cracking is not load associated, but is caused by a combination of dry shrinkage and temperature differentials. Shrinkage cracking in cement treated pavements is usually a direct result of material failure when the tensile stresses induced by shrinkage exceed the tensile strength of the material. High strength pavements may exhibit wide cracks at relatively wide spacing while a pavement layer stabilized with lower cement contents are likely to exhibit finer cracks at closer spacing (5).

Loss of water through evaporation, self-desiccation during the hydration of the cement, and temperature differentials are known to cause shrinkage of cement treated materials (5, 6, 7, 8). Whether the resulting cracking affects the structure and performance of the pavement depends on the ability and availability of water to penetrate the base through the cracks, the resistance of the material to abrasion and degradation in the presence of water, and the nature of the subgrade material (9, 10, 11).

Reflection Cracking

Reflection cracking is best described as the appearance of cracks at the surface of the HMAC that mirror those cracks in a lower pavement layer. Shrinkage and thermal cracks that develop in the cement treated pavement layers and then propagate through the surface layer form reflection cracks. Reflection cracking is usually non-structural because it does not in itself reduce the life of the pavement; however, the combined effect of traffic and the environment can lead to premature failure. The predominant cause of premature failure is water infiltration. Most cracks in CTB pavements are not "hairline", most will permit water to enter the base layers. This infiltration is more serious in winter months due to thermal contractions of the CTB. Water infiltration can lead to the following problems:

i) in a CTB pavement water can infiltrate the reflection cracks and this can cause debonding and loss of pavement fines through pumping, leading to premature failure;

ii) wetting of the subgrade reduces its elastic modulus, and this will lead to an increase in the tensile strain of the upper layers;

iii) wetting of the base and subbase reduces its elastic modulus and thus increases the tensile strain in the HMAC surface; and

iv) in colder climates, water trapped in cracks can undergo a freeze-thaw cycle and effectively widen cracks to increase failure probability.

v) on pavements built on expansive clays this wetting can lead to pavement swells around the cracks.

Thermally Induced Stresses

Thermal stresses develop due to temperature changes caused by daily and seasonal variations in ambient and ground temperatures. A hardened CTB changes volume with change in temperature and decreases in length with a decrease in temperature. The temperature susceptibility increases with an increase in cement content and an increase in density (7). Thermal stresses in an uncracked cement treated pavement are significant and usually large enough to initiate cracking (8).

Laboratory tests performed on highly compacted specimens of lean concrete gravel showed low strength values and high modulus values at early stages of curing (13). These high modulus values increase the stresses at early stages of curing. The high tensile stresses induced by the temperature changes are usually greater than the low initial strength of the stabilized material and the formation of cracks is therefore unavoidable. Cracks in the stabilized layer can propagate through the asphalt layer to the surface. This increases the danger of water penetration and subsequently also the possibility of pumping of fines and cement from the stabilized layer.

Pumping of Fines

The distress known as pumping can be defined as the rapid release of a pressurized soil-water mixture from a relatively high to a relatively low pressure potential, whereby surface material may be redistributed in different directions (10). Normally the pressure is released vertically through joints, cracks, and edges. These vertical cracks may be load-induced fatigue cracks or drying and thermally induced cracks. It is therefore important to

minimize and prevent any vertical cracks that can lead to pumping. Research has shown (5) that overstabilization of poor quality material and material with large amounts of fines can lead to an increase in the amount of drying and shrinkage cracks that will develop during curing.

Normally the following conditions should be present for pumping and erosion to take place:

a) upper layer deflection associated with voids or weak interlayers within or between different layers,
b) sufficient water within the layers or at the interlayers, and
c) materials that are susceptible to pumping and erosion.

Poor Drainage

Several case studies have been reported that investigate the effect of poor drainage on the pavement structure under accelerated testing performed with the South African Heavy Wheel Simulator (HVS) (10). It was observed that different material types behave differently under excessive porewater pressure. The following is a brief discussion of the effects that poor drainage has on the different layers of a pavement structure.

Bituminous layers are usually insensitive to water under pressure, but if cracked they can undergo stripping and delamination. However, some older asphalt mixtures containing rounded river gravels are particularly prone to stripping. Granular layers can experience an increase in density if the initial compaction was performed poorly. The higher the confining pressure, the greater the strength of the granular material. The higher the density, the lower the permeability and the more difficult it is for water to infiltrate the layer (9, 10). This additional compaction will be felt as increased roughness by the road user.

Cement stabilized layers are generally insensitive to water under pressure (10). However, these layers can become more sensitive to pumping due to the effects of traffic and the environment; in extreme cases the material can revert to a state that is equivalent to that of an unstabilized granular material. Weakly cemented materials of lower quality and fine grading tend to erode more easily (10). Coarser grained material can form advanced

cracking and crushing if the parent rock is highly weathered. In the crushed state the risk of shear failure is similar to that of granular materials. This deterioration and crushing occurs around cracking in the surfacing, the end result is a significant increase in road roughness.

FAILURE MECHANISM

A single factor or a combination of the above mentioned factors can lead to premature failure of a cement treated pavement. A description of one potential failure mechanism for CTB's with thin surfacings is presented in this section. This mechanism could involve layer debonding, shrinkage, and thermal cracking reflecting through the surface layer, which would allow water to infiltrate the underlying layers. Figure 2.1 illustrates a proposed mechanism (17), it can be described as follows:

i) the base layers cracks due to thermal and other non-loading stresses;
ii) the top of the CTB layer erodes in the wheelpaths under the action of traffic in the presence of water;
iii) debonded interfaces of layers give way to water, which in turn aggravated the effect of debonding by further reducing the friction between layers (this leads to pumping of fines and movement of water between layers);
iv) longitudinal cracking of the upper CTB occurs in the wheelpaths due to reduced support and increased strain; and
v) finally the pavement breaks up from the top to the bottom.

The prevention of this type of failure mechanism should not only consist of the reduction or prevention of reflection cracking but also the ability to maintain a waterproof barrier to prevent water from infiltrating the CTB. The prevention of pumping of fines is vitally important to the preservation of the pavement structure and load carrying capability.

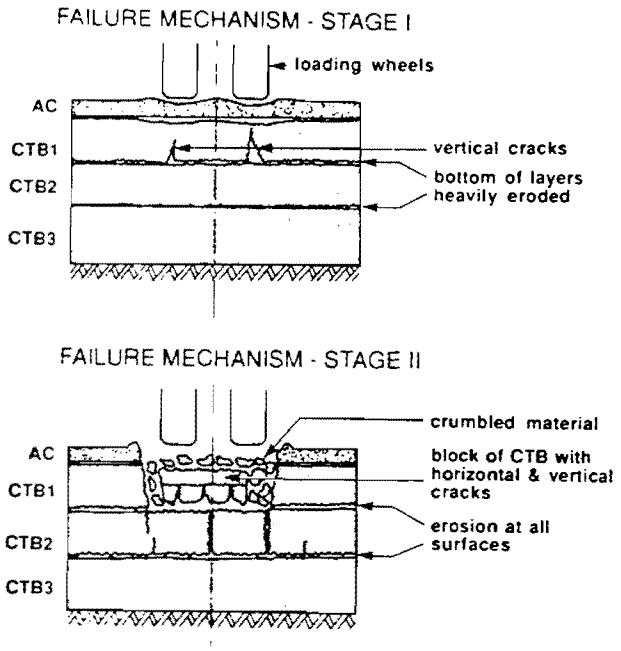

Figure 2.1. Failure of a Three Layer CTB Pavement (Kadar et al., (17)).

CODE OF PRACTICE AND STANDARD SPECIFICATIONS

Most road authorities use a code of practice or specification to guide engineers in their use of stabilized materials. This practice is important because it will decrease the use of improper road building materials and methods. The following is a brief discussion of the recently reported research performed and codes of practices developed to predict durability and performance of stabilized pavements.

Shrinkage Tests

Tests were performed research in Australia (5) on cement treated materials that led to the following important findings.

a) The proportion of clay fines influences the drying shrinkage potential. The shrinkage potential increases with increase in the plasticity index.

b) The type of clay mineral present influences the drying shrinkage potential, with the smectite group causing the highest shrinkage.

c) Cement content also influences the shrinkage potential. However, this influence appears to decrease with increase in material quality.

d) The use of a low cement content with poor quality materials is likely to result in significant drying shrinkage.

e) The linear shrinkage of the fine fraction of the aggregate was identified as being a very good indicator of the eventual drying shrinkage potential of a cement treated material.

This research and other field work completed in Australia (5) led to a change in standard specifications. The specifications were subsequently changed to include:

a) a maximum linear shrinkage of 1.5 percent is allowed;

b) a maximum plasticity index of 4.0 percent is allowed;

c) fly ash blend cement as a stabilizer is introduced;

d) reduction of the percentage of fines passing the 75 μm sieve to an allowable maximum of 7 percent are reduced; and

e) shrinkage test in which a control beam of cement treated base could not exceed 250 microstrain shrinkage after 20 days is introduced.

Cracking patterns observed in the field after implementation of these specifications were at the regular 5 to 7 meter interval, but noticeably finer (5). Variations in construction techniques included the placing of a bitumen seal over the CTB for 6 months before applying the asphalt surface layer to remove any premature cracking due to drying shrinkage. These measures, together with experience gained at Queensland Department of Transportation, provide the road construction industry with a better technical understanding of the reflection cracking problem and the means currently available to treat the problem.

South African Erosion Test

The South African erosion test device was developed to evaluate the durability of a cemented material in the laboratory. The aim of erosion testing is to identify fine grained materials that are susceptible to erosion so that they may be avoided or modified. The remainder of this section will introduce this test. Chapter 3 and Appendix A contain a more detailed discussion of the procedures and equipment.

In the erosion test, three rectangular specimens are submerged in water and covered with a rough neoprene membrane. The membrane has a contact texture of very rough sandpaper. A 17.775 kg wheel with a bevelled rim is rolled over the sample to erode the surface. After 5000 repetitions the depth of erosion is measured at 15 points on the specimen surface. The erosion index is expressed as the mean of the average depth of erosion for the three specimens. The main advantage of this is that at present this is the only test that reasonably simulates the actual erosion action that takes place in the field on a cement treated base layer in the presence of water.

Existing Erosion Tests (Wet and Dry Durability Tests)

Presently, in the USA, two wet and dry durability tests are used to determine the erosion resistance of cement treated materials. The first is a mechanical wet and dry test that measures the percentage of material that is lost after 12 wetting and drying cycles. During each cycle the specimen is rotated at 60 rev/min for 50 cycles. A stationary 2.25 kg brush erodes the specimen surface. The second test is known as the hand wet and dry test and is similar to the mechanical test, except that in this test the cylindrical specimen is smaller and is eroded with a hand held brush. For the mechanical test modified AASHTO compaction as opposed to proctor compaction is used. Two brush strokes of approximately 13.5 N each are applied over the curved surface of the specimen between each cycle.

The main difference between the above mentioned tests is that the erosion test simulates the grinding action of pavement layers in the presence of slight water pressure whereas the durability test simulates the loss of cementation due to continued wet and dry cycles in a pavement by brushing the sample. An extensive evaluation and comparison of these two tests has been given elsewhere (10). The South African wheel tracking device

was favored because it more closely simulates field conditions, and it was found to be better at predicting eventual performance in accelerated pavement testing studies with the heavy vehicle simulator.

Strength Test

Presently, the Texas Department of Transportation uses a strength requirement as a standard specification for the construction of cement treated pavements. The strength requirement is a minimum design compressive strength of 5170 kPa with an allowable cement content between 4 and 9 percent; this is TxDOT design strength L. Design strength M requirement is a minimum compressive strength of 3450 kPa with an allowable cement content between 3 and 9 percent. The compressive strength on the laboratory prepared samples is tested in accordance with Test Method Tex-120-E.

Unconfined compressive strength tests or soaked unconfined compressive strength tests are performed on cement treated materials to determine the strength of the material. This is probably the most widely used test method for designing cement treated materials. Research and field studies performed in South Africa showed that adequate strength and durability can be obtained from materials treated with 2 and 3 percent cement (10). However, these materials should have low fines and plasticity index values. Research performed in Australia (5) on the shrinkage potential of cement treated materials emphasized the importance of upgrading specifications to address this problem, thus ensuring a better understanding of cement treated materials. It is therefore hypothesized that too much emphasis is placed on satisfying strength criteria and not enough consideration is given to a better understanding of the shrinkage and durability aspects of treated materials. There should be a balance between the amount of stabilizer used and shrinkage potential of the material in order to alleviate shrinkage and still meet strength requirements.

TYPICAL TRENDS OBSERVED WITH THE EROSION TEST

Laboratory test results were reported for the South African wheel tracking device on four types of relatively fine-grained materials (10). These materials were regarded as substandard and had to be stabilized before they could be used in road construction. Figure

2.2 shows the sieve gradations of the four types of materials. Erodability testing was done with the erosion test, and the specimens cured in special steel chambers for seven days at 70 degrees Celsius and a relative humidity of 100 percent. Figure 2.3 illustrates the increase in erosion depth with the number of repetitions for the four materials at various compaction densities. The figure indicates a non-linear increase in erosion depth with increase in repetitions for lower densities. This is a direct result of the increase in effective area or contact area of erosion. The erosion index (L) is the average depth of erosion after 5000 load repetitions of the wheel on the specimen in the erosion test device. The effect of density on the erodability of a material is illustrated by applying the erosion index (L) on the erosion results (Figure 2.3). Figure 2.3 illustrates the decrease in erosion index (L) with an increase in compaction density. Only materials 3 and 4 showed relatively low erosion at densities greater than 95 percent. Materials 1 and 2 showed high erosion irrespective of their high compaction densities. Other researchers (11) have reported that inadequate compaction may cause erosion to increase by a factor of 5. The erodability characteristics of stabilized fine-grained materials can be drastically improved with an increase in compaction density. It is therefore clear that on-site quality control for density of lightly cemented materials must be applied accurately and consistently.

SUMMARY

1) The increased use of cement treated materials resulted from a number of factors, including the depletion of quality paving material resources, increase in traffic volume and load, as well as the need to construct high performance pavements on poor subgrades and/or high water tables.
2) Stabilizing the upper layers increases the stiffness of these layers and provides increased support and load spreading capabilities.
3) Cement stabilized pavements have proven to be an effective and economical alternative to conventional full depth flexible pavements. However, cement stabilized pavement will crack and form block cracks shortly after construction.

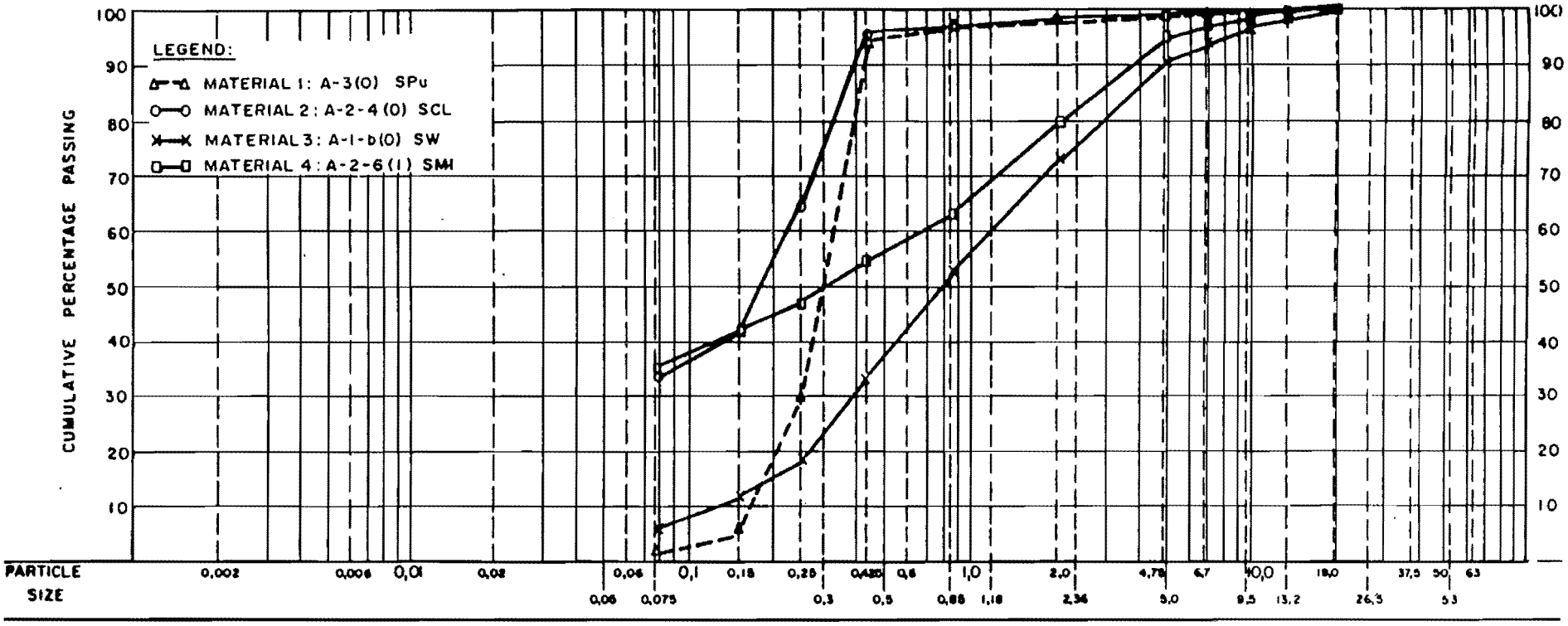

Figure 2.2. Sieve Gradings of Fine Grained Materials Used (10).

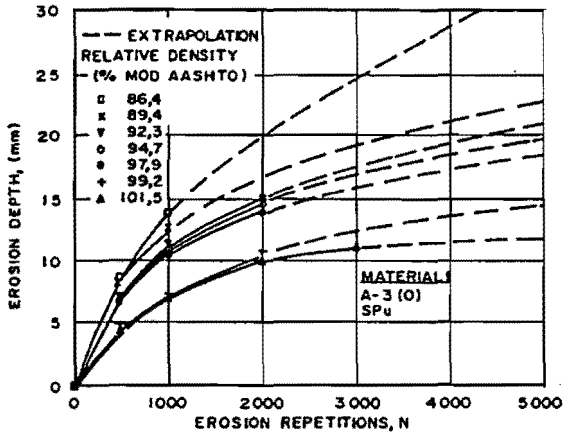

(a) MATERIAL 1: UNIFORM SAND + 4 % PBFC

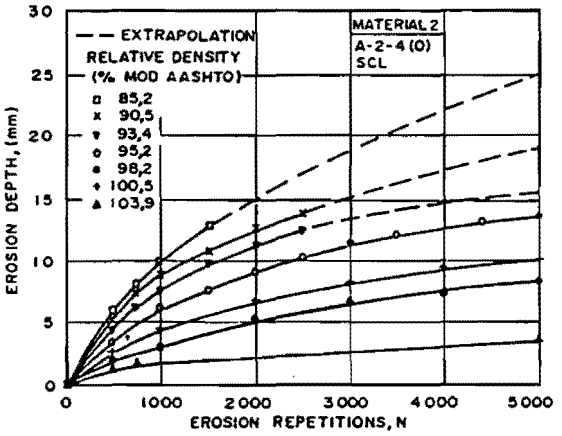

(b) MATERIAL 2: VERY CLAYEY SAND (LOW PLASTICITY) + 4 % LIME

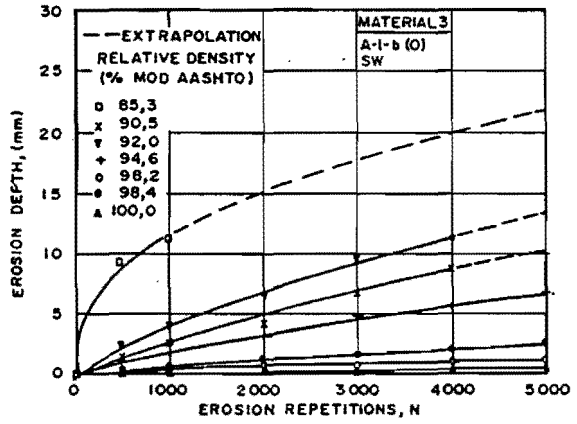

(c) MATERIAL 3: WELL GRADED SAND + 4 % PBFC

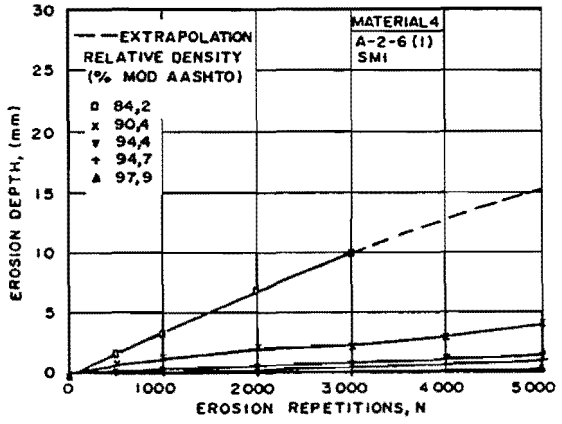

(d) MATERIAL 4: VERY SILTY SAND OF INTERMEDIATE PLASTICITY + 4 % LIME

Each individual result represents the average of three test specimens, 15 measurements per specimen.

Figure 2.3. Increase in Depth of Erosion at Various Compaction Densities with Number of Repetitions of Materials Used (10).

Performing multiple tests and changing specifications accordingly to address these problems can minimize problems resulting from this cracking.

4) Shrinkage cracks will eventually reflect through the surface layer. Whether or not the reflection cracks seriously affect the structural integrity and performance characteristics of the CTB pavement is largely dependent on the ability and availability of water to infiltrate the cracks, resistance of the cemented material to erosion and degradation in the presence of water, and the nature of the subgrade material.

5) Research performed in Australia showed that the linear shrinkage test was a good indicator of drying shrinkage potential for cement treated material. A better technical understanding of the reflection cracking problem and upgrading the specifications in Australia led to improvements in the performance of the cement treated materials.

6) Research performed in South Africa showed that the South African erosion test can be used to evaluate the durability of fine grained cement treated material in the laboratory. Incorporating this test with other tests can assist in more effectively addressing and evaluating durability problems.

7) CTB design relies too heavily on strength requirements. Strength may or may not correlate to eventual field performance. More work is needed to balance strength with other performance related factors such as cracking and durability.

CHAPTER III: MATERIAL AND TEST DESCRIPTION

INTRODUCTION

The following discussion describes the different types of materials and tests used to evaluate the durability of the cement treated materials from the Houston District. The material used in the stabilized base on SH 36 consisted of a crushed limestone treated with 6 percent cement. This aggregate together with crushed limestone from different locations was used in the laboratory testing to evaluate the durability of a cement treated material.

As part of the research effort of this project, the following tests were performed:

a) Atterberg limits (plasticity index, liquid limit, plastic limit),
b) soaked U.C.S. test,
c) South African erosion test (10), and
d) shrinkage test.

This chapter discusses each of these tests in detail. Furthermore, the purpose of this chapter is to provide a detailed description of the engineering properties of the materials used in the test program. Each material was obtained from a different source and is described in terms of gradation and Atterberg limits. These materials were used in the above mentioned tests to predict strength, linear shrinkage, and possible durability problems.

MATERIALS DESCRIPTION

General

The first material (herein referred to as material A) used for testing is a crushed limestone from the Houston district. This material was reported to be the same material that was used in the construction of SH 36. However, after evaluation of this material it was found that the gradation and PI values of the fines were different from the original material used on SH 36. Material A had less clay and fine particles and is generally a better quality material than the material used in SH 36. The original material was reported to have a PI of 9, whereas material a was found to have a PI of less than 2.

Material B was a crushed limestone sample from a stockpile near the Bryan/College Station area. It was found that this material had no plasticity and was therefore expected to perform well as a stabilized material. Since material B had no plasticity, it was decided to modify this material by adding clay fines. This modified material (herein referred to as material C) was used to compare different quality crushed limestone materials. The modification of material B consisted of the addition of clay fines until a plasticity index of 7.4 was reached.

The plasticity index of 7.4 is well within the range allowed by TxDOT specifications. These specifications require a plasticity index value of less than 10. Materials B and C were used to determine the effect of different gradations and plasticity index values for the tests performed after cement stabilization. Each of the three materials were treated with cement. Three different levels of cement content were used, namely 2, 4, and 6 percent cement by weight.

Insitu samples were also taken from SH 36 and cut into beam specimens to be tested with the South African erosion device. After performing the test no erosion was evident; however, a large amount of clay was observed in the insitu samples. The clay in the insitu samples varied in size and clay particles with a diameter of 25 mm. Figure 3.1 illustrates the cement treated base layer with the clay particles visible.

Hydrometer Test Performed on Original Base Material

Approximately 500 grams of the fine material, passing the 2 mm sieve size, from the original aggregate were used to perform a hydrometer test. ASTM D 422:63 describes the hydrometer analysis used to determine the percentage clay present in the original aggregate. Soil particles smaller than 0.002 mm in size are classified as clay according to definition. From the test results, it can be concluded that the clay present in the original aggregate is approximately 12.5 percent.

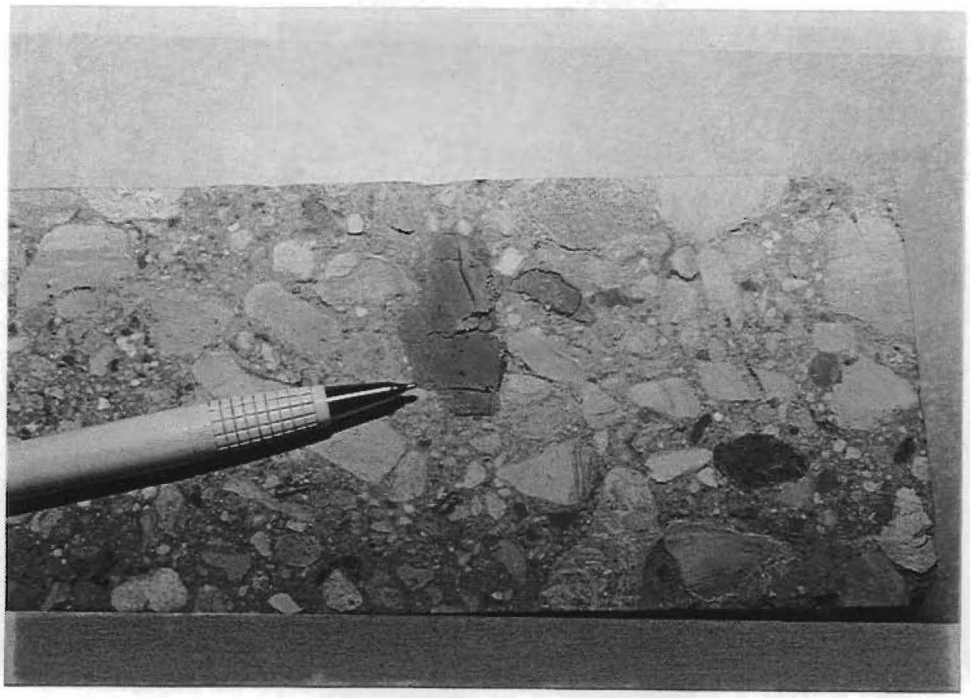

Figure 3.1. Clay Particles Present in the In situ Material Taken from SH 36.

Gradation and Maximum Dry Density

Figure 3.2 shows the gradation of each of the three material types. For the purpose of this report, only the material passing the 9.4 mm sieve diameter size was used. The reason for this is that the erosion test was designed for the testing of fine grained material with a maximum diameter size of 19 mm.

The optimum moisture content at maximum dry density for the three materials was determined by using the modified AASTHO method. The specimens were mixed and compacted at optimum moisture content. The maximum dry density was used to calculate the dry weight of the material needed in molding the beam specimens: Appendix A shows an example of this calculation. Table 3.1 describes of the engineering properties of the different materials.

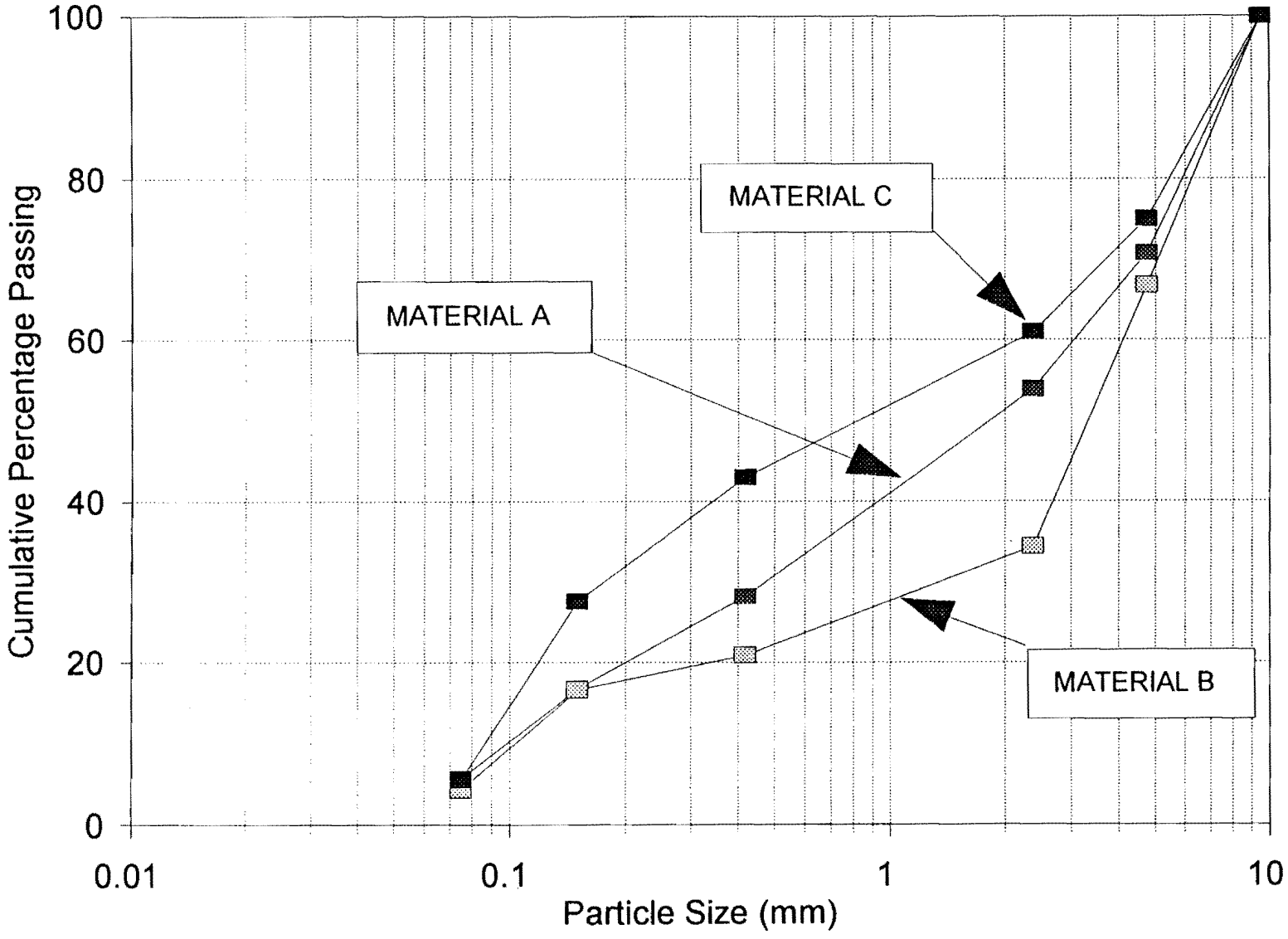

Figure 3.2. Sieve Gradings of the Three Materials Used in the Study.

Table 3.1. Description of the Three Materials Used in the Laboratory Tests.

Crushed Limestone	Material A	Material B	Material C
% passing 420 μm	28.1	20.9	43.0
% passing 75 μm	5.6	4.3	5.5
Plasticity index	2.9	Non-Plastic	7.4
Liquid index	14.25	-	15.70
Plastic limit	17.25	-	23.10
Optimum moisture content (kg/m^3)	2175.3	2360.0	2308.0
Maximum dry density (%)	7.6	8.2	8.8

DESCRIPTION OF LABORATORY TESTS

General

The amount of fines present in a stabilized material will greatly affect the performance of this material under the above mentioned tests (5). The amount of fines present in the material will also affect the shrinkage properties and plasticity index, and this will directly affect the durability of the stabilized material. It is therefore important to determine the percentage fines and plasticity index of the materials used. By reducing the amount of fines and the plasticity index, the shrinkage potential of a material can be greatly reduced and the durability increased (5). The type of clay fines passing the 420 μm sieve size will affect the plasticity index, and the amount of fines present will affect the durability.

Erosion Test (South African Wheel Test)

The objectives of this alternative erosion test method were as follow:

1) to provide a relatively quick assessment of the erodibility of fine grained cementitious materials, but not excluding coarse materials;
2) to simulate flexible behavior in the wet state during pumping;

3) to include aggregate to aggregate contact stresses that may initiate surface crushing (compressive failure) on the specimen to produce erodible (pumpable) free fines; and

4) to provide a test based on the depth of erosion (rather than the weight loss) of the specimen.

The main difference between this erosion test and existing erosion tests is the way in which the free fines are produced from both aggregate-to-aggregate contact and water at the surface of cemented layers within the pavement, since the hydrolic characteristics of the water alone do not produce surface erosion.

Figure 3.3 illustrates a schematic diagram of the erosion test device, and the Appendix provides a detailed layout. The device consists of a loaded wheel running on a linear track along the top side of the erosion specimen. The specimen is encased in gypsum in a smaller steel container that is placed in a water bath. Three specimens can be tested simultaneously in the bath, which is sealed at the top with a flexible neoprene membrane. Three friction pads are secured underneath the membrane and are in direct contact with the specimen. This provides the aggregate-to-aggregate contact stresses at the surface while the wheel moves over the specimen.

The test is performed underwater on a soaked specimen, with the friction pad and loading as the main eroding action to produce free fine aggregates. The water is slightly pressured in order to remove the free fines under the loaded wheel path. Appendix A gives a detailed description of the erosion test method and device. Table 3.2 contains a summary of the relevant information on the test device.

The friction pads are made from commercially available Silicon Carbide crystals of 1.0 mm (16 mesh). The erosion specimens are manufactured in the laboratory. They can also be sawed from in situ layers. The method used to prepare the laboratory specimens is described in detail in Appendix A. During this research both in situ and laboratory specimens were prepared and tested to determine the amount of erosion of each sample.

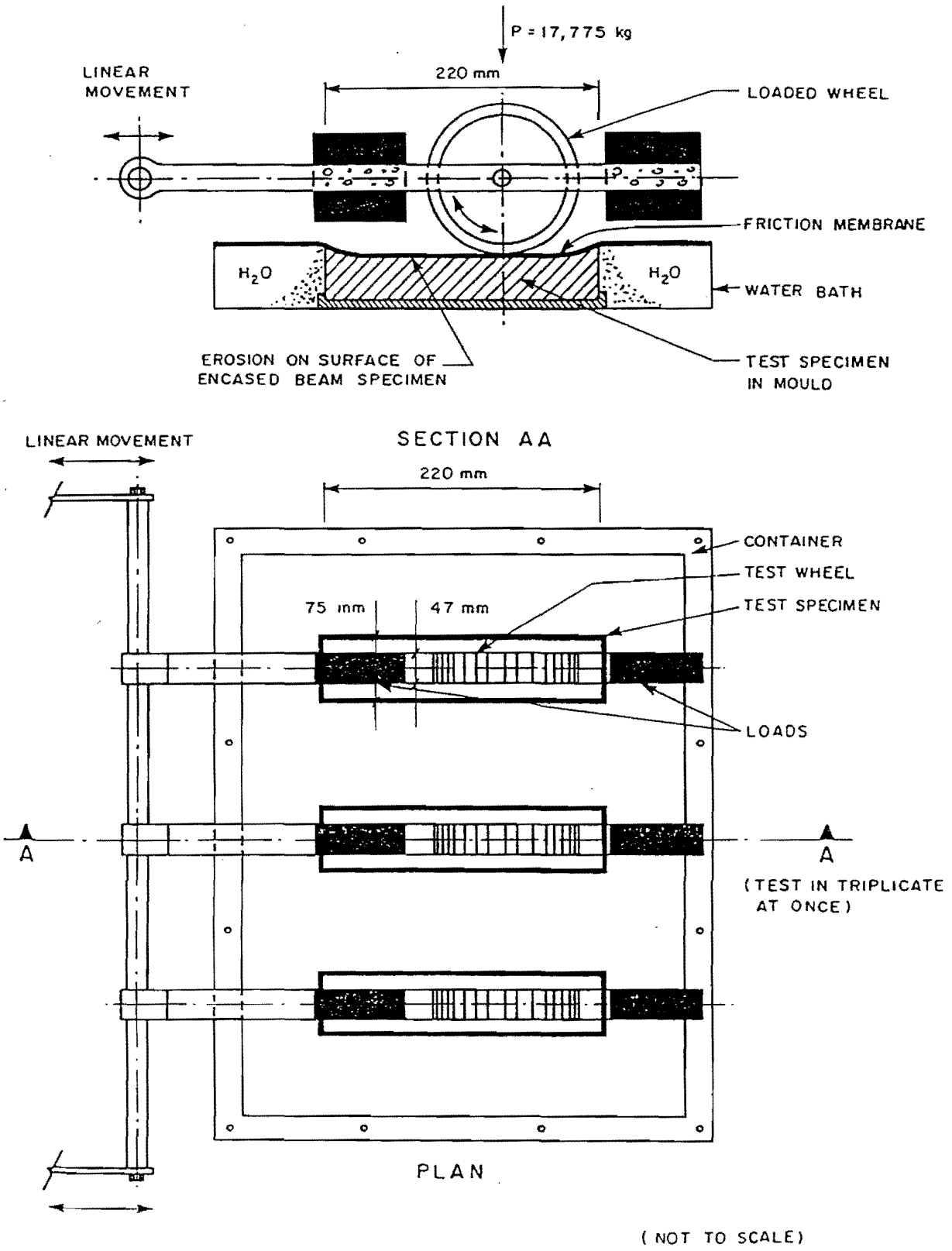

Figure 3.3. Schematic Diagram of the Erosion Test Device.

Table 3.2. Detail Information of the Erosion Test (10).

Load cycle frequency:	1 Hz
Testing length:	220 mm
Length of specimen:	+/- 270 mm
Height of specimen:	Variable, fixed to same height at start of each test
With of specimen:	75 mm
Maximum aggregate size:	+/- 19 mm
Total load per wheel:	17.755 kg
Contact stress (dry state):	1.0 to 2.2 MPa
Width of wheel:	47 mm
Diameter of wheel:	205 mm
Size of friction pad:	75 mm x 270 mm
Aggregate on friction pad:	1.0 mm (16 mesh) silicon crystals
Number of cycles before measurements:	Variable, normally 5000 cycles to determine erosion index

The laboratory specimens were prepared in a mould to produce specimens with approximate dimensions of 75 mm by 75 mm by 450 mm. These beam specimens were used to measure linear shrinkage in the longitudinal direction. The shrinkage test will be discussed later in this chapter. After completing the shrinkage measurements, the beam specimen was sawed using a water cooled diamond blade saw. Cubes of 75 mm were sawed from each end of the beam specimen to be used in unconfined compressive tests.

The erosion measured in the erosion test can be reported either as the weight loss of the specimen or as a percentile value of the overall depth of erosion. However, it was found that measuring the depth of erosion is more accurate than determining the weight loss and serves as a better indication of the erosion (10). Figure 3.4 illustrates the measurements necessary to determine erosion depth. The erosion depth is measured with a Vernier calliper at specific positions of a measuring jig at three locations across the specimen and five locations along the length of the specimen. Fifteen measurements are taken on the specimen before and after the specified number of load repetition are applied. Care should be taken to ensure measurement positions before and after testing is the same. Appendix A describes this procedure in more detail.

The erosion test was performed on three materials which will be described in this chapter as well as samples taken from State Highway 36. Specimens from material A were cured for seven days in a special chamber at 70°C before testing. This is an accelerated curing method (10). Because this curing method was used no shrinkage measurements were taken, since the specimens were placed inside a steel chamber. Appendix A describes this curing method in detail. Specimens from materials B and C were cured under controlled environmental conditions for 21 days before performing the erosion tests. These specimens were cured at 25°C and 90 percent relative (for consistency) humidity and shrinkage measurements were taken from these specimens.

Shrinkage Test

Beam specimens were manufactured in the laboratory from materials B and C after treating each material with 2, 4, and 6 percent cement. The treated material was mixed at optimum moisture content and compacted to 95 percent Modified AASHTO density. The specimens were dynamically compacted in three equal layers and 56 blows per layer were applied with a modified AASHTO hammer (4.54 kg). The specimens were then compressed five times in a press to a maximum load of 275 KN in order to obtain maximum density and an even surface (this procedure is described in detail in Appendix A). The specimen was then taken out of the mould and placed in a controlled environment for 24 hours. Gauge studs were securely attached to each end of the specimen with an epoxy glue. The

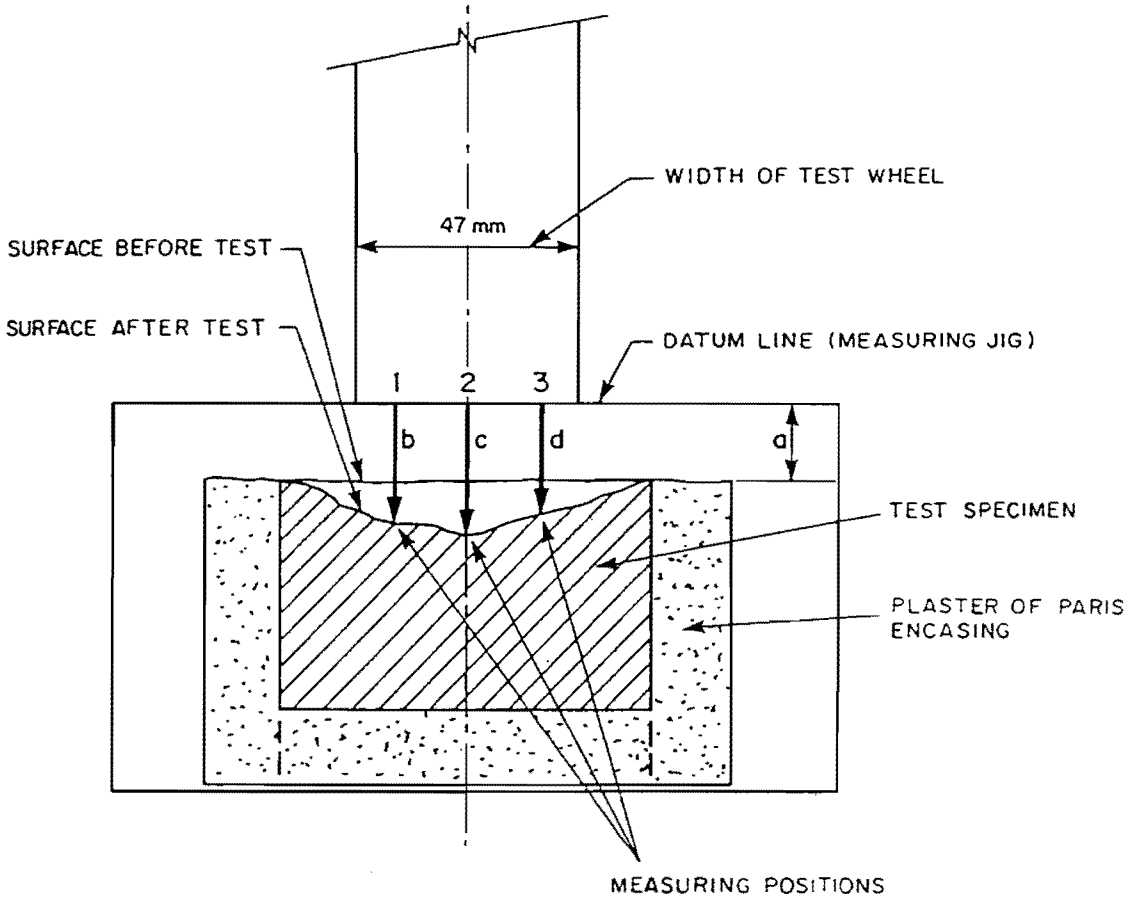

Figure 3.4. Measuring of the Erosion Depth with a Vernier from a Fixed Point.

first measurement was then taken with a digital Vernier with an accuracy of 0.01 mm. The specimens were left for 21 days in the controlled environment, and measurements were taken at regular intervals. For the purpose of this research the controlled environmental conditions were at 90 percent relative humidity and 25°C. These conditions can be changed to reflect actual field conditions for a specific test material. The largest amount of shrinkage takes place in the first few weeks (5) and to ensure a short testing period the measurements were only taken during the first 21 days. The micro-strain is calculated for the samples of length 4500 mm over the period of 21 days.

Unconfined Compressive Test (UCS)

UCS tests were performed on cubes obtained from beam specimens of the three materials after each were treated with 2, 4, and 6 percent cement by weight. The end parts of a beam specimen were sawed after taking the final shrinkage measurements at a length of 75 mm to produce a cube 75 mm by 75 mm by 75 mm. The procedure used for compaction and molding of the different beam specimens is also described in detail with examples of calculations in the Appendix. Each cube was soaked for 3 hours before being tested until failure. A constant loading rate of between 20 and 40 kg per second was applied until failure, and the load at failure was then recorded.

CHAPTER IV: RESULTS AND DISCUSSIONS

GENERAL

This chapter presents the results of the laboratory evaluation of the test materials described in Chapter 3. The following laboratory tests were performed: UCS test, shrinkage test, and erosion test for three different materials. The results were analyzed to predict possible durability problems with the cement treated material used to construct the base and subbase layers of SH 36.

GRADATION AND ATTERBERG LIMITS

Figure 3.2 shows the gradation for the three materials and the percentage fines passing the 420 μm sieve size for each material. This data shows that Material C has the greatest amount of fines passing the 420 μm sieve, a total of 43 percent, and a plasticity index of 7.4. Material A had a plasticity index of 2.9, and Material B was non-plastic. The Atterberg limits and the maximum dry density at optimum moisture content for the three materials are shown in Table 3.1. After analyzing the gradation and Atterberg limits, it was expected that Material C would perform the poorest in the above mentioned tests because Material C consisted of a large amount of fines and had the highest plasticity index of the three materials tested. Materials A and B showed a better particle distribution and less fines; therefore, these materials could be labeled as better quality materials.

UNCONFINED COMPRESSIVE STRENGTH TEST (UCS)

Table 4.1 shows the soaked unconfined compressive strengths for the three materials after treatment with 2, 4, and 6 percent cement by weight. The UCS test was performed on these materials to determine the percentage of cement at which the requirements for both strength and durability are met. Therefore, it was also important to determine if lower percentages of cement could be used with satisfactory results. The test cubes were soaked for 3 hours before performing the UCS test. Different curing methods were used for the materials to evaluate the practical implications of each method. The beam specimens for Material A were cured for 7 days in special steel chambers at 70°C.

Table 4.1. Unconfined Compressive Strength at Failure for the Three Materials Used in Laboratory Testing.

Cement contents	Material A (kPa)	Material B (kPa)	Material C (kPa)
2 %	6500	3380	1170
4 %	8070	5200	3100
6 %	10070	7300	4200

The beam specimens for Materials B and C were cured for 21 days in controlled environmental conditions of 90 percent relative humidity and 28°C. The second curing method is preferred since linear shrinkage measurements could be taken more easily at different intervals of the test, although this method is more time consuming. Chapter 3 describes these test methods in detail.

At present the Texas Department of Transportation is using a strength requirement as a standard specification for the construction of cement treated pavements. The design strength L requires a minimum UCS of 5170 kPa with an allowable cement content between 4 and 9 percent. Design strength M requires a minimum UCS of 3450 kPa with 3 to 9 percent cement contents. The UCS values are taken after 7 days of curing according to Test Method Tex-120-E. The design strength for the stabilized base layer of SH 36 (for consistency) was specified to be a minimum of 4140 kPa. The results shown in Table 4.1 indicate that Material A, with 2 percent cement treatment, had an average strength of 6500 kPa after 7 days of accelerated curing. This is more than 50 percent higher than the specified design strength for SH 36. It should be noted that the curing method used to obtain the results shown in Table 4.1 was different from the specified TxDOT method. Also the UCS was performed on cubical and not cylindrical specimens as in the TxDOT Method Tex-120-E. It is therefore recommended that more research work be performed to determine the effect of the different curing methods on the UCS of the samples. However, the high strength obtained from Material A with a cement contents of 2 and 4 percent seems to indicate that adequate strength can be obtained with lower cement contents by limiting the amount of plasticity fines in the material. Therefore, the cement content for treatment

of better quality materials can be decreased to 2 and 3 percent while strength requirements are still met. This will be a more cost effective design and a good potential for future cost savings.

SHRINKAGE TEST

Shrinkage tests were performed on materials B and C to determine the factors that influence the shrinkage potential of cement treated materials. These two materials were used to evaluate the influence of the amount of fines and the plasticity index on cement treated materials. Material B was non-plastic with 20.9 percent fines passing the 420 μm sieve, and material C had a plasticity index of 7.4 with 43 percent fines passing the 420 μm sieve.

Figures 4.1, 4.2, and 4.3 illustrate the effect of the shrinkage potential in micro-strain for the two materials at different percentages of cement content. In evaluating these results it is useful to compare them to the Australian criteria of a maximum of 250 microstrain after 20 days. Figure 4.1 shows the increase in shrinkage potential with an increase in plastic fines. This is illustrated by the higher shrinkage potential of material B after 21 days of curing. The slope of the shrinkage measurements taken for material C is much steeper and demonstrates a faster increase in shrinkage over time. Figure 4.1 shows an increase in the shrinkage potential with an increase in the plasticity fines for the two cement treated materials. The plastic fines strongly influences the shrinkage potential. However, this effect will decrease with an improvement in the quality of the material. The results show that the shrinkage potential increases with an increase in the fines of the cement treated material.

The same trend is illustrated in Figures 4.2 and 4.3 as was observed from the previous results. The greatest factors affecting the shrinkage potential of a cement treated material appear to be the amount of fines and the plasticity fines in the mix.

The shrinkage versus time for the two materials at 2, 4, and 6 percent cement content is illustrated in Figures 4.4 and 4.5. The 2 percent cement content showed a higher shrinkage potential than the 4 and 6 percent for material B. This trend was also observed by other researchers (5). However, the 6 percent cement mix deviated from this trend by not showing the lowest shrinkage potential. A possible explanation is that the influence of the cement content is less prominent for better quality materials, and future research is

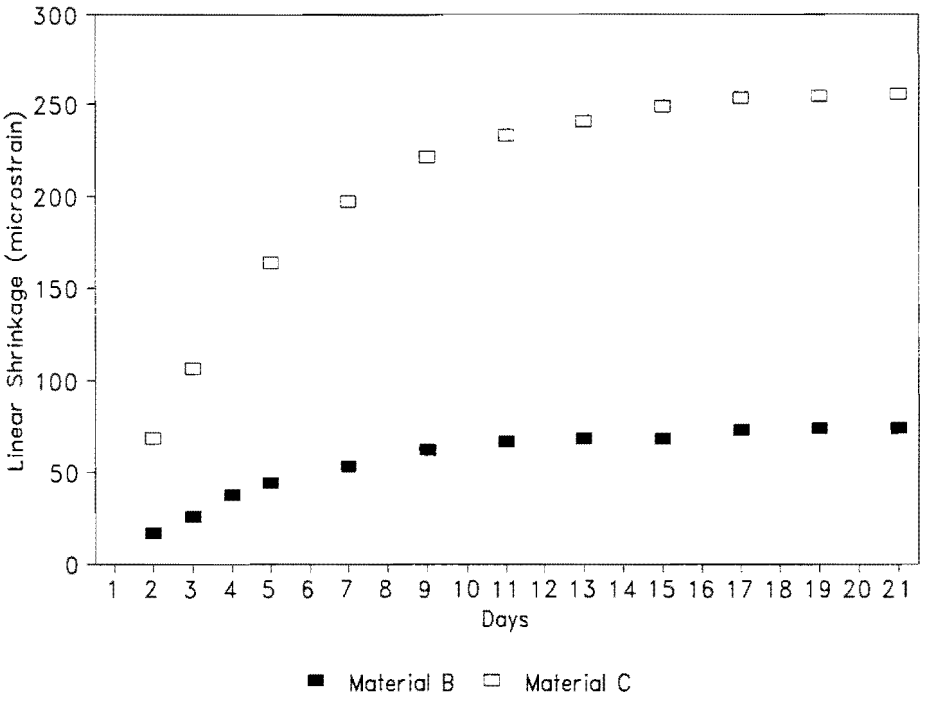

Figure 4.1. Materials B and C with 2 Percent Cement Content.

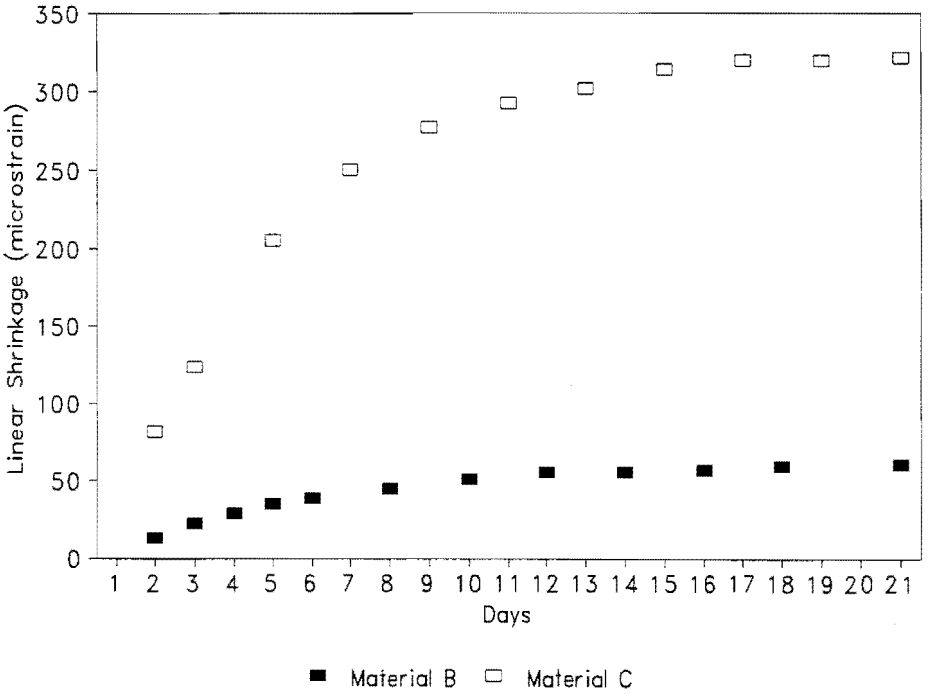

Figure 4.2. Materials B and C with 4 Percent Cement Content.

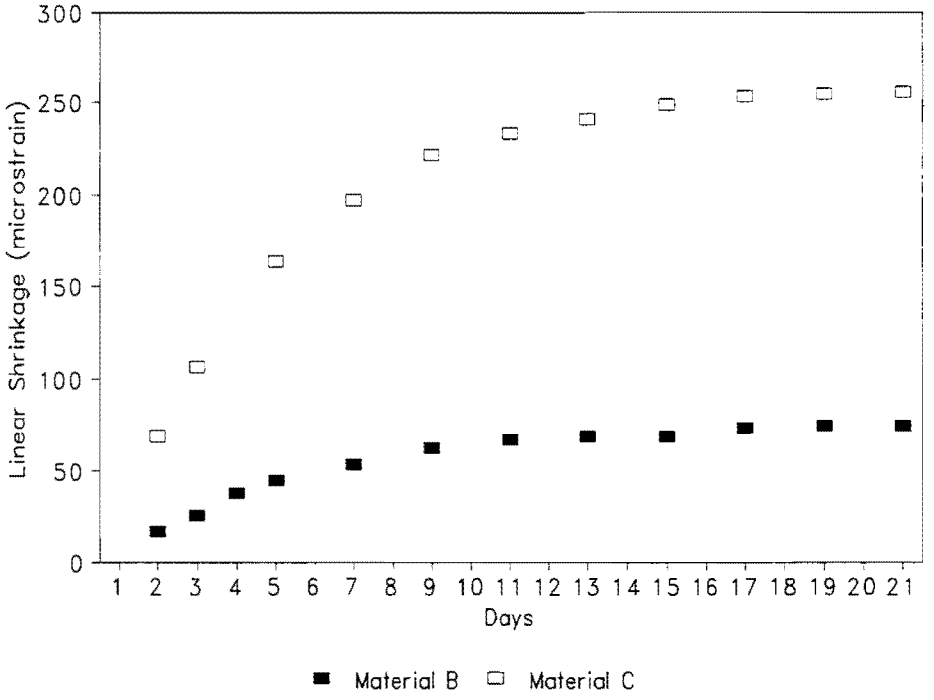

Figure 4.3. Materials B and C with 6 Percent Cement Content.

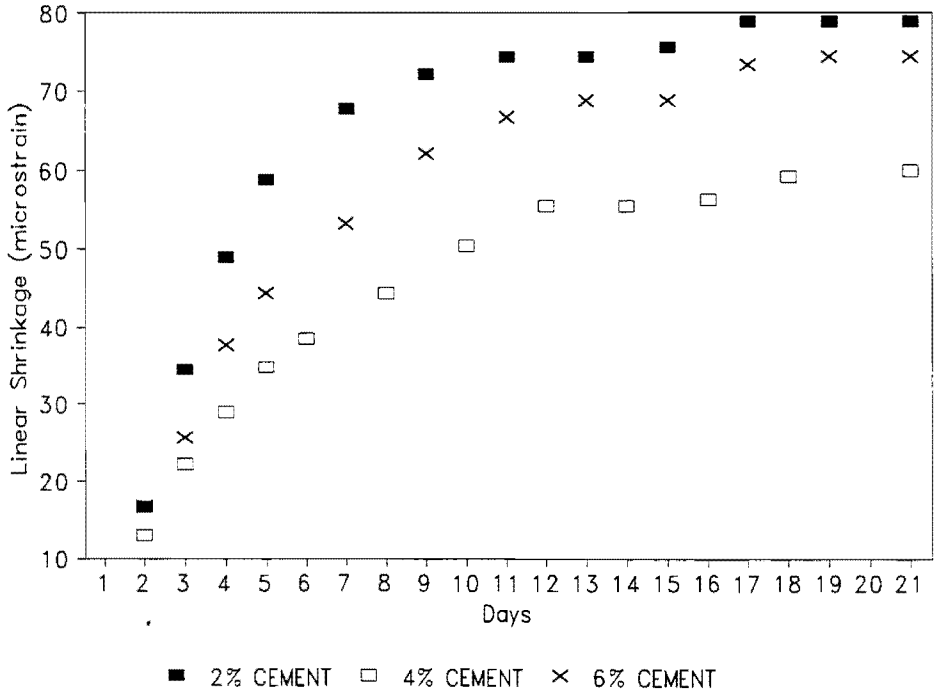

Figure 4.4. Material B with 2, 4, and 6 Percent Cement Content.

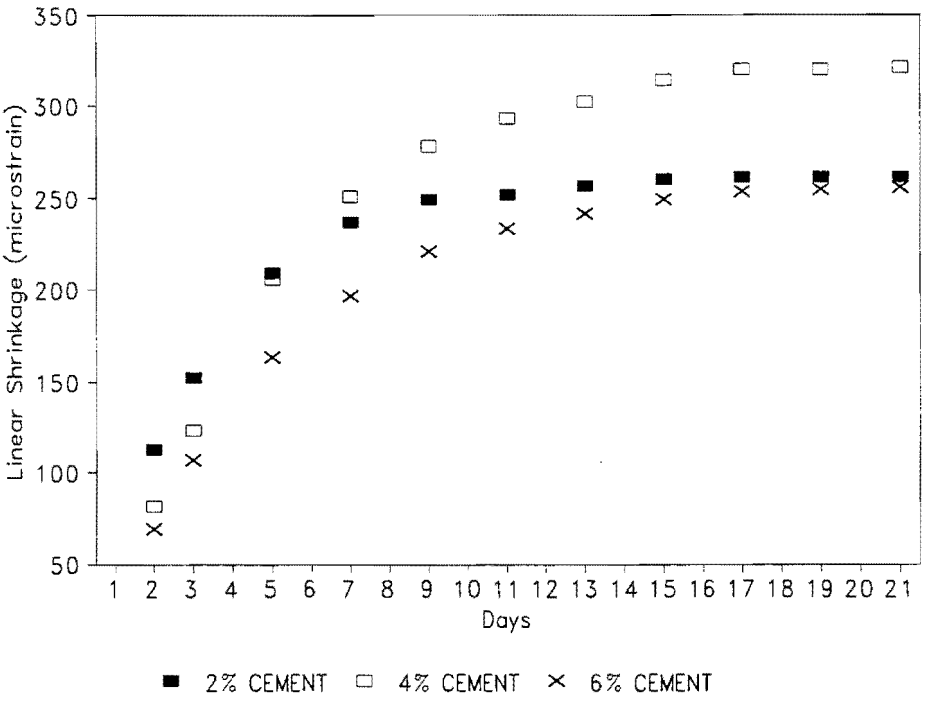

Figure 4.5. Material C with 2, 4, and 6 Percent Cement Content.

recommended. Several issues need to be resolved such as the variability of test results from duplicate samples. However, the important issue is that the overall shrinkage of all three samples was substantially less than interia recommended by other researchers, i.e., 250 microstrain (5). The difference in shrinkage potential after 21 days between the largest and smallest values were relatively small (20 microstrain). This may indicate that the use of better quality materials can reduce the effect that cement content has on shrinkage potential.

The results in Figure 4.5 exhibit a similar trend for the shrinkage potential at different cement contents. However, the 2 percent mix did not follow this trend. No explanation for this was found, and future research is recommended. The shrinkage potential is most severe in the case of material C, which had a poor gradation and a larger amount of fines passing the 420 μm sieve. This is illustrated by the difference between the largest and smallest values of the total shrinkage measured for material C (80 microstrain). This value is four times greater than the value measured for material B. The results indicate that the use of

relatively low cement contents with poor quality material is likely to result in significant drying shrinkage.

The results indicate that material B at the three different percentages of cement content will pass the Australian specifications. This specification specifies an allowable maximum linear shrinkage of 250 microstrain after 21 days of curing. However, material C did not pass this specification and showed linear shrinkage values equal to and greater than 250 microstrain after 21 days of curing. Figures 4.4 and 4.5 show material B passing and material C failing the linear shrinkage specifications. It can therefore be anticipated that the use of material C will lead to the development of a high amount of shrinkage and reflection cracking.

EROSION TEST

The erosion test was performed on the three sampled materials as well as on samples taken from SH 36. The samples taken from SH 36 were tested and showed no erosion. During the test on the field samples, it was observed that the erosion wheel rolled over the larger aggregates, which prevented erosion of the finer particles. The South African erosion test was designed for fine grained base materials with a maximum diameter of 19 mm. The samples taken from SH 36 consisted of base material with aggregate sizes larger than 30 mm, which prevented erosion from taking place during the test. Therefore, in subsequent laboratory tests, only the material passing the 9.5 mm sieve size was used for the three test materials. After performing the test on materials A and B at different cement contents, no significant erosion was determined, as shown in Figure 4.6. Figure 4.6 shows materials A and B with no fines eroded from the samples after 5,000 cycles; therefore, the original surface texture is still shown after performing the erosion test. The same results were obtained from materials A and B at different percentages of cement content, therefore showing no erosion taking place during erosion testing of these treated base materials. The results indicate that materials A and B are durable, and high strength materials would not be prone to erosion and pumping of fines.

In the case of material C, the erosion wheel rolled over the larger aggregates, preventing erosion of the aggregate particles from taking place. Erosion depths of 1 to 2

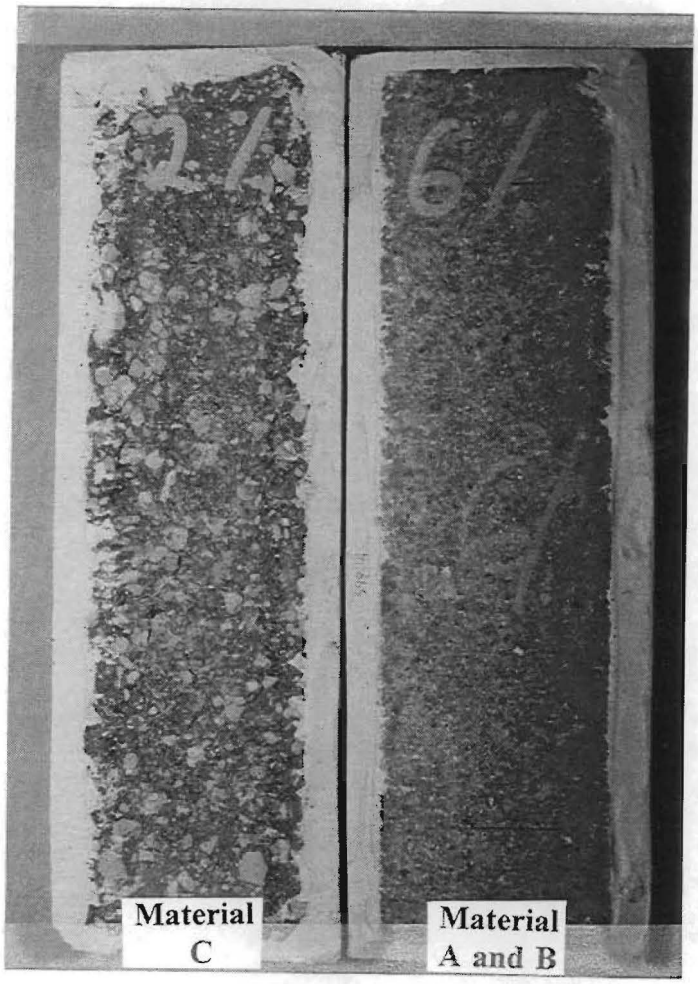

Figure 4.6. Material C with 2 Percent Cement and Materials A and B with 6 Percent Cement are Shown After Performing the Erosion Test (5,000 Cycles).

mm were measured; however, with the South African classification this material would have excellent durability resistance. Figure 4.6 clearly shows the aggregates from material C more exposed than materials A and B; therefore, some amount of fines were washed out from the material C sample. This exposed the aggregates of the test sample, but the large size of the aggregates prevented any measurable erosion from taking place. These results stress the fact that it is important to determine a maximum aggregate size for the test material to ensure usable test results. Further research work is recommended in this field

to determine the effect that wet and dry cycles or freeze and thaw cycles would have on the sample materials before performing the erosion test. These cycles could then simulate actual field conditions to ensure a better understanding and evaluation of the treated base material. The test equipment was found to be a very effective tool if used on fine grained cement treated base materials with no large aggregates. However, the use of this equipment seems to be confined to fine materials, since no erosion was measured for the coarse material specimens that were tested.

SUMMARY

The following conclusions can be made from the laboratory tests performed on the cement treated materials:

1) The use of lower cement contents with better quality materials than those currently used showed acceptable strength development. It is recommended that the fines content of the stabilized material be more strictly controlled.
2) The plasticity index of the clay fines, as well as the type of clay mineral, strongly influences the shrinkage potential. The results show that the shrinkage potential increases with an increase in fines and plasticity index.
3) The cement content of the stabilized material influences the shrinkage potential. However, this effect decreases with an increase in material quality.
4) Linear shrinkage appears to be a good indicator of the shrinkage potential of cement treated material.
5) The South African erosion test could be a very effective tool if used on fine grained cement treated materials.

CHAPTER V: SUMMARY OF FINDINGS AND RECOMMENDATIONS

This project was aimed at identifying the cause of the rapid deterioration of the cement treated base on State Highway 36 near Orchard, Texas. The base consisted of two cement treated layers (CTBs) one on top of the other, the top CTB layer was found to have completely disintegrated in the wheel paths after only 2 years in service. An initial evaluation was performed in 1994, and several contributing factors were found to be involved including:

a) the high percentage clay in the top CTB layer, and
b) the placement of the new CTB on top of the stabilized recycled old pavement, which resulted in shrinkage cracks that reflected to the surface but stopped at the lower stabilized layer.

This placement of different stabilized layers on top of one another resulted in debonding of the layer and moisture getting trapped at the layer interface. However, the initial problem was concentrated in the wheel paths as cores taken from the shoulder showed little deterioration. It was initially proposed that the top CTB had eroded primarily due to the mechanical action of traffic. This assumption turned out to be false.

To investigate the erodibility issue, a review was made of available erodibility procedures and recommendations were made to test the SH 36 materials with a modified South African wheel tracking procedure. The modifications include measuring not only erosion but also shrinkage potential and compressive strength from the same beam sample. Block samples from SH 36 were taken and tested in the laboratory together with manufactured samples containing the SH 36 coarse aggregates with varying quality of fines. In these manufactured samples the cement content was varied from 2 to 6 percent. The results obtained from the erosion test device indicated that even with the lower quality fines at the low stabilized content erodibility was not a problem with any of these materials tested. These results lead to the conclusion that mechanical erosion was not the main cause of the durability problems found on SH 36. Subsequent work presented in a companion

report (2919-2) found that the likely cause of the deterioration was probably linked to a chemical erosion (carbonation).

Interesting observations from the test results were:

a) the shrinkage results clearly show the influence of the higher plasticity fines on shrinkage potential and presumably eventual layer cracking of the CTB; and
b) with the usual good quality aggregate used in the Houston District it appears possible to reduce the amount of stabilizer and meet strength requirements while maintaining adequate durability.

The South African wheel tracking device and modified test procedure show potential for establishing the optimum stabilizer content for any base material. This is important as TxDOT uses more and more non-conventional materials. The existing TxDOT specifications focus on compressive strength. This can lead to problems with these materials as high stabilizer contents are required to meet strength requirements. However, at this level of stabilization undesirable shrinkage cracking usually occurs. Future design considerations should include shrinkage and durability as well as strength.

REFERENCES

1. Murphy, H.W., and E. Con. Shrinkage Cracking of Cement Treated Bases. Main Roads Department Queensland, Research Report 88072M054E, Queensland, Australia, 1986.
2. Little, D.N. Fundamentals of the Stabilization of Soil with Lime. Published by the National Lime Association, Arlington, Virginia, 1987.
3. Little, D.N. Handbook for Stabilization of Pavement Subgrades and Base Courses with Lime (Final Draft). Sponsored by the National Lime Association, Arlington, Virginia, 1994.
4. Yoder, E.J., and M.W. Witczak. Principal of Pavement Design (2nd Edition).
5. Rawlings, R.E. Drying Shrinkage of Cement Treated Paving Materials (Thesis). University of Queensland, Australia, 1988.
6. George, K.P. Cracking in Soil Cement. Australian Road Research Board Proceedings, Vol.7, Part 7, 1974, pp. 38-53.
7. Highway Research Board Bulletin 292. Soil Stabilization with Portland Cement. National Academy of Science - National Research Council, Publication 867, 1961.
8. Otte, E. Thermal Affects in Cemented Pavement Layers. The Highway Engineer, Vol. 25, Number 12, 1978, pp. 2-8.
9. Van Wijk, A.J., and C.W. Lovell. Prediction of Subbase Erosion Caused by Pavement Pumping. Transportation Research Record 1099, TRB, National Research Council, Washington D.C., 1986, pp.45-57.
10. De Beer, M. Aspects of Erodibility of Lightly Cementitious Material. Division of Roads and Transport Technology, CSIR, Pretoria, South Africa, 1989.
11. Phu, N.C., and M. Ray. The Hydraulics of Pumping of Concrete Pavements. Bulletin de Liaison des Laboratoires des ponts et Chaussees, Special Issue 8 (in French), 1979, pp. 15-31.
12. Williams, R.I.T. Cement Treated Pavement Materials: Design and Construction. Elsevier Applied Science Publishers, London and New York, 1986.

13. Marais, C. P., Otte, E. and Bloy, L. A. K. The Effect of Grading on Lean-Mix Concrete. Highway Research Record 441, Washington, 1973, pp. 86-96.
14. Lytton, R.L., J. Uzan, E.G. Fernando, R. Rogue, D. Hiltunten, and S.M. Stoffels. Development and Validation of Performance Prediction Models and Specifications for Asphalt Binders and Paving Mixes. Report SHRP-A-357. Strategic Highway Research Program. National Research Council, Washington, D.C., 1993.
15. Huang, Y.H. Pavement Analysis and Design. Prentice Hall, Englewood Cliffs, New Jersey, 1993.
16. Texas Department of Transportation. Standard Specifications for Construction and Maintenance of Highways, Streets, and Bridges. Adopted by the Texas Department of Transportation, 1995.
17. Kadar, P., E. Baran and R.G. Gordon. The Performance of CTB Pavements Under Accelerated Loading - The Beerburrum (Queensland) ALF Trail 1986/887. ARRB Research Report ARR No. 158, 1989.

APPENDIX

DETERMINATION OF THE EROSION INDEX OF CEMENTITIOUS MATERIALS

[The following appendix is taken from research performed by De Beer et al. (10) to outline test procedures and apparatus of the South African erosion test.]

A.1 SCOPE

This method describes the procedures for determining the erosion index, L, of the cementitious materials using the erosion test device in which water saturated beams of cementitious materials are tested under repetitive loading. This is known as the erosion test method.

A.2 APPARATUS

A.2.1 Apparatus for soil preparation

A.2.1.1 Sieve 19 mm

A.2.1.2 Riffler with 25 mm spacings, 800 mm long

A.2.1.3 Plastic bags (460 mm x 300 mm)

A.2.1.4 Plastic bags (900 mm x 550 mm)

A.2.1.5 Oven (0 - 200 celsius)

A.2.1.6 Aggregate crusher (to reduce aggregate to minus 19 mm)

A.2.1.7 Basins (400 mm x 125 mm deep)

A.2.1.8 Balance (0 - 10 kg)

A.2.1.9 Shovel

A.2.2 Apparatus for mixing of materials

A.2.2.1 History sheet (see Figure A.1)

A.2.2.2 Basin (400 mm x 125 mm deep)

A.2.2.3 Scoop

A.2.2.4 Flask (500 ml)

A.2.2.5 Distilled water (+/- 500 ml per specimen)

A.2.2.6 Balance (0 - 10 kg)

A.2.2.7 Plastic bags (460 mm x 300 mm)

A.2.3 Apparatus for production of specimens

A.2.3.1 Static loading facility (+/- 275 kN) with minimum bottom plate dimensions of 200 mm x 500 mm

A.2.3.2 Compaction mould (see Photo Plates A.1 and A.2)

(i) Two side plates

(ii) Two end plates

(iii) Top and bottom plate

(iv) Four high tensile steel rods 510 mm long with threaded ends, M17

(v) Four steel M17 nuts and washers

(vi) Metal bar (449.5 mm x 74.5 mm x 85 mm)

(vii) Two handling rods (120 mm x 5 mm diameter)

(viii) Metal spacer strips :

(a) Two of 520 mm x 25 mm x 20 mm

(b) Two of 520 mm x 25 mm x 10 mm

(c) Two of 520 mm x 25 mm x 5 mm

(ix) Mould extension (see Photo Plate A.3)

(x) Fiber based phenolic resin base plate (448.5 mm x 25.4 mm x 74.5 mm)

(xi) Four rubber spacers (40 mm x 25 mm x 35 mm)

A.2.3.3 Vernier caliper (0 - 150 mm, in mm)

A.2.4 Apparatus for accelerated airing

A.2.4.1 Stainless steel container (460 mm x 80 mm x 120 mm)

A.2.4.2 Container cover with silicone rubber seal

A.2.4.3 Four M5 wing nuts

A.2.5 Apparatus for cutting of specimen

A.2.5.1 Water cooled diamond saw cutting facility

A.2.6 Apparatus for mounting of specimen

A.2.6.1 Stainless steel mounting tray (300 mm x 95 mm x 27 mm deep)

A.2.6.2 Tray extensions (75 mm high)

A.2.6.3 Two clamps

A.2.6.4 Tray extension supports

A.2.6.5 Flask (2000 ml)

A.2.6.6 Spatula

A.2.6.7 Gypsum (calcium sulphate, $CaSO_4.1/2H_2O$) approximately 1.25 kg for each specimen

A.2.6.8 Waterproof marking pen

A.2.7 Apparatus for unconfined compressive strength (UCS)

A.2.7.1 Loading facility as in A.2.3.1

A.2.7.2 Vernier caliper (0 - 150 mm)

A.2.7.3 Test result form as in TMHl, method A14, form A14/1

A.2.8 Apparatus for erosion testing

A.2.8.1 Erosion test device (see Photo Plate A.4)

A.2.8.2 Neoprene rubber membrane (520 mm x 445 mm x 3 mm thick)

A.2.8.3 Membrane retaining frame (see Photo Plate A.5)

A.2.8.4 Six stainless steel specimen tray clamps (flat plate 45 mm x 30 mm x 5 mm with 10.5 mm diameter hole at center)

A.2.8.5 Four clamps

A.2.8.6 Friction pads (one for each specimen)

A.2.8.7 Six M10 stainless steel Allen screws 25 mm x 40 mm

A.2.8.8 M10 Allen key wrench

A.2.8.9 Three spacers (perspex sheets 30 mm x 95 mm x 25 mm thick)

A.2.9 Apparatus for preparation of friction pads

A.2.9.1 Norton P80 Tuffback Purite wet or dry abrasive paper (280 mm x 230 mm)

A.2.9.2 Silicon Carbide Crystolon grit (crystals), 1 mm (16 mesh) (+- 30 grams for each friction pad of size 75 mm x 220 mm)

A.2.9.3 Pliobond (500 ml)

A.2.9.4 Acetone (500 ml)

A.2.9.5 Glass beaker (80 ml)

A.2.9.6 Glass beaker (400 ml)

A.2.9.7 Paint brush (25 mm)

A.2.9.8 Plastic bags (250 mm x 200 mm)

A.2.9.9 Clipboard and waste paper (300 mm x 250 mm)

A.2.9.10 Stanley trimmer knife

A.2.9.11 Stainless steel mounting tray (as in 2.6.1)

A.2.9.12 Steel rule (400 mm)

A.2.9.13 Scale (0 - 1 kg)

A.3 APPARATUS FOR MEASUREMENT OF DEPTH OF EROSION

A.3.1 Measuring jig (see Photo Plate A.9 later on)

A.3.2 Vernier caliper (0 - 150 mm)

A.3.3 Erosion test sheet (see Figure)

A.3.4 Balance (0 - 10 kg)

A.3.5 Phenolthalene (500 ml)

A.3.6 Hcl (5 N diluted, 500 ml)

A.4 METHOD FOR PREPARATION OF EROSION SPECIMENS

A.4.1 Soil preparation

Air dried is treated in accordance with TMH1 method A7 to establish maximum dry density and optimum moisture content.

A.4.2 Mixing

A.4.2.1 The required mass of raw material as calculated from example shown in Section A.6 is placed in a large basin (400 mm x 125 mm deep).

A.4.2.2 Stabilizing material is added and thoroughly mixed with the dry raw material.

A.4.2.3 The calculated quantity of distilled water is added while mixing thoroughly.

A.4.2.4 The required mass of wet mixture is weighed out into a plastic bag (mass of bag added) sealed, and left for 30 minutes.

A.4.2.5 Material is remixed by manipulation, in situ, in the sealed bag.

A.4.3 Compaction mould preparation

A.4.3.1 Semi-floating mould preparation:

(i) The clean mould is assembled and placed over the bottom plate, which, with the use of four rubber spacers (each spacer 40 x 25 x 35 mm jig compresses approximately by 16 mm at 2 kN load) placed between the mould and bottom plate at the four corners, allows the male portion of the bottom plate to enter the mould by +/- 5 mm. See Photo Plate A.6.

(ii) A 25.4 mm thick fabric-based phenolic resin specimen support plate (448.5 mm x 75 mm x 25.4 mm), mass previously recorded, is placed on top of the bottom plate to facilitate specimen handling on completion. Support plates are numbered and are used to identify specimens until they are mounted in trays. The numbered trays will then serve this function.

(iii) The inner surfaces of the mould and top and bottom plates are sprayed with a release agent (WD40). Excess release agent is mopped up with paper toweling. A mould extension is used to fill the mould with all the mixed material in one operation.

A.4.3.2 Dynamic and static mould preparation

Rubber spoons are not used. Preparation is identical to semi-floating in all other respects.

A.4.4 Compaction of the specimens

Rubber spacers are not used. Preparation is identical to semi-floating in all other respects.

A.4.4.1 Static compaction

(i) The predetermined (as in Section A.6) mass of mixed material from the plastic bag is poured and spread evenly into the mould to fill it. If necessary, tamp the material with a spatula or use metal bar (449.5 x 74.5 x 85 mm) to settle it below the level of the extension. See Photo Plate A.2 (b). Remove the extension from the mould.

(ii) Two metal spacer strips (as in Section A.2.3.2 (viii)) 1 x 20 mm and 1 x 10 mm thick (total of 30 mm either side) are placed on top of the mould. The top plate is then positioned with the male portion entering the mould.

(iii) The mould assembly is positioned in the center of the loading facility and the metal bar (as in Section 2.3.1(vi)) placed on top to distribute the load to be applied. A load of 20 kN is applied and released; then the 20 mm thick spacers between the mould and top plate are removed. A load of 90 kN is applied and released. The remaining metal and rubber spacers are removed. The mould should now be handling on the specimen, supported only through friction between the specimen and cycled five times to attain maximum density. Section A.4.5 describes how the mould is then removed and dismantled.

NOTE: It is unlikely that Max. Dry Density (MDD) will be attained by the compaction effort, which is found to be less than the MDD attained by the AASHTO method (from which the required mass of material is calculated). However, should 100% MDD be attainable, spacers compensate for the 25.4 mm thickness of the specimen support plate will need to be introduced to prevent the specimen being compressed to less than 75 mm thickness, i.e. more than 100% MDD (modified AASHTO).

A.4.4.2 Dynamic compaction (Mod. AASHTO)

After mixing, the required mass of material for the specimen is equally divided by mass into three separate plastic bags.

The compaction mould is marked at 14 positions 30 mm apart. See also Photo Plate A.3 (a).

Using a Mod. AASHTO hammer, the specimen is compacted in three layers as follows:

(i) Material from one bag is evenly spread into the mould, which is standing on a concrete floor.

(ii) The hammer is positioned at the first reference point against one side of the mould and allowed to fall freely from its maximum height. It is then moved to the next adjacent reference point. This process is repeated for all points (total 14) along this one side and is repeated along the opposite side. Total blows on this first layer are now 28. A repeat on this layer is now done to give a total of 56 blows on this first layer.

(iii) The second and third layers are similarly treated. The mould extension is now removed, and the top plate placed on the mould with the male portion entering the mould.

(iv) As in Section A.2.3.1, the metal bar is placed on top and the whole unit positioned in the static loading facility, and a maximum load of 275 kN is applied and cycled five times to obtain maximum density and an even surface on the specimen.

A.4.5 Removal and curing of specimen

A.4.5.1 Support the compaction mould by introducing spacers between the mould and bottom plate. This is to prevent the sides of the mould from slipping down and possibly damaging the specimen when dismantling.

A.4.5.2 The top plate is removed and mould dismantled by removing retaining bolts and tapping the end plates outward. (The side plates of the mould must be held in position because they tend to separate from the specimen of their own accord when the end plates come free.) Remove side plates.

A.4.5.3 The exposed specimen resting on the support plate is removed as a unit and massed. The previously recorded mass of the support plate is subtracted and specimen mass and a means of three measurements for length, width, and height are recorded on specimen history sheet.

A.4.5.4 For normal curing, the specimen (still resting on support plate) is placed in the humidity room and protected by plastic sheeting placed over it.

A.4.5.5 For accelerated curing, the specimen (still resting on support plate) plus excess water (approximately 70 ml) is sealed in the stainless steel container as in

Section A.2.4.1 (460 mm x 80 mm x 120 mm internal diameter) and placed in an oven at 70 - 75°C for a period of seven days. See Photo Plate A.6. All details of storage, date made, etc. are recorded on the specimen history sheet (see Figure A.1).

A.4.6 Erosion testing procedure

A.4.6.1 Preparation of test specimen (third point loading and erosion or UCS)

After the curing, as described in the previous section, the beam specimens (450 mm x 75 mm x 75 mm) are removed and allowed to cool slowly for approximately two to three hours. If third point loading tests (Otte, 1972, 1978) are also to be done, the beam specimens (450 mm x 75 mm x 75 mm) are used for this purpose.

After the third point loading test, the larger piece of specimen is used for erosion testing. The smaller piece is cut into 75 mm cubes for soaked unconfined compression strength (UCS) testing. If only erosion testing is to be done, two equidistant pieces (leaving 270 mm center portion for erosion specimen) are cut from the ends of the beam specimens to be used for UCS testing. See Photo Plates A.7 and A.8.

A.4.6.2 Moulding of erosion specimen with gypsum

Mix sufficient gypsum and water to ensure a creamy mix (approximately 1.25 kg per specimen). Pour the mixture into a specimen tray and place the specimen equidistantly within the tray with the top of manufactured specimen uppermost. There should be sufficient mix so that the specimen will displace the mix to fully fill the tray and extension. If necessary, add extra mixture with a spatula to accomplish this. After the gypsum has set, remove the extensions and clean gypsum from sides of tray. Write the specimen number at the left-hand corner of any long side of tray using waterproof permanent ink. Submerge specimens in water and enter details (where stores, date mounted, etc.) on relevant specimen history (see Figure A.1).

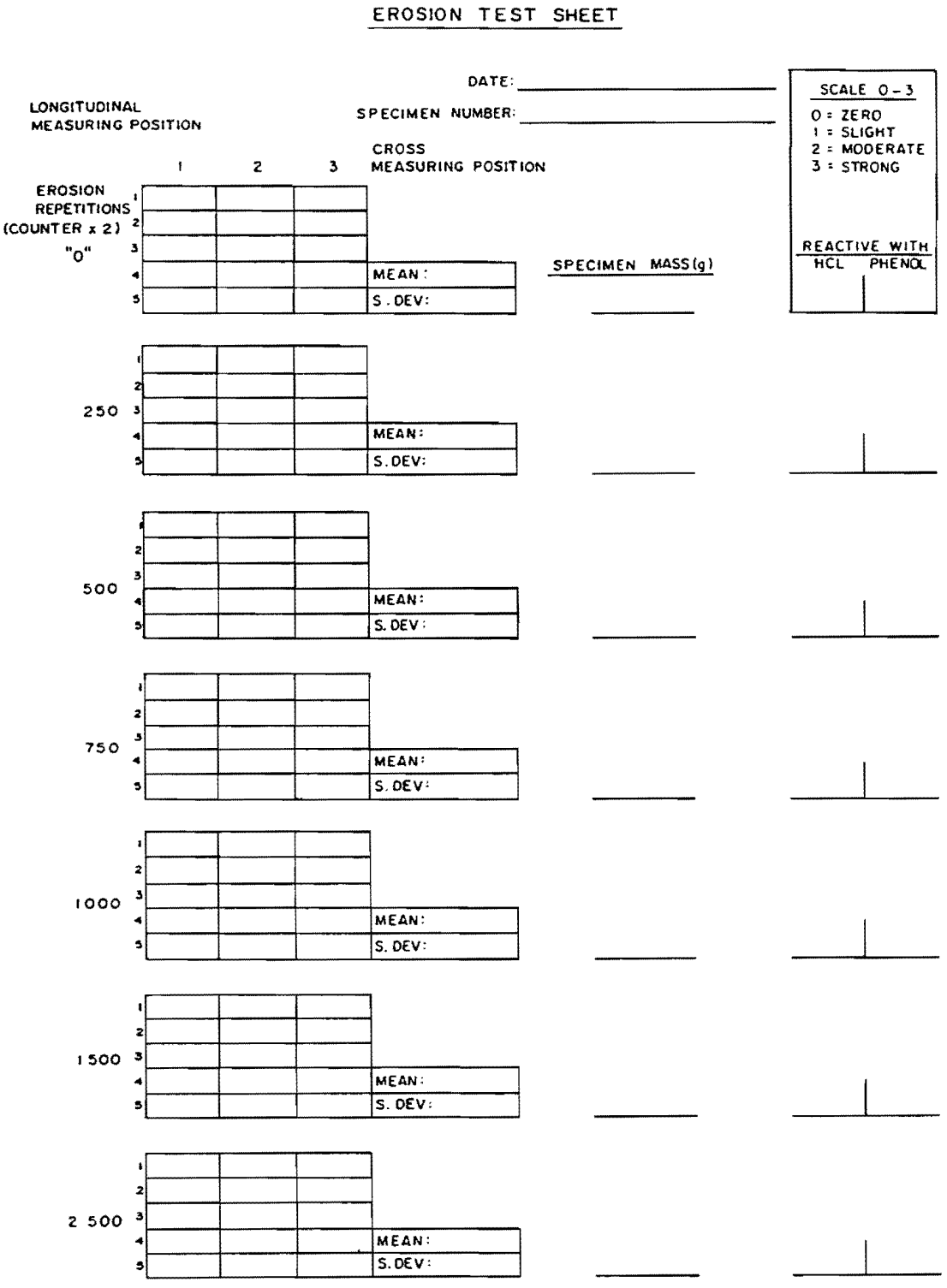

Figure A.1 Data Sheet for Erosion Test Results.

A.4.6.3 Preparation of the surface of the erosion specimens

(i) Owing to the possible effects of carbonation (Netterburg, 1984) on the surface of the specimens (just prior to testing), the specimens are cut to the wanted thickness so as to remove the carbonated layer. Specimens may be cut to a thickness of 75 mm, 50 mm or 27 mm (measured from bottom of tray).

(ii) The specimens are cut with a diamond saw blade and water so that the cut surface is parallel to the bottom of the tray in which it is mounted. See Photo Plate A8.

NOTE: The particular field of interest being investigated will determine the cutting thickness; for example, if the surface of an in situ stabilized layer is carbonated, a block of cemented material is removed from the road and cut to produce erosion specimens of the required thickness leaving the carbonated surface intact so that the effects of carbonation on erosion can be studied.

(iii) Wash the surface of the specimens under running water to remove loose particles, then immerse in water until no further gain in mass is recorded (soaked).

(iv) Remove excess water with a moist cloth and weigh the specimens.

(v) Test with phenolthalien and HCl reaction. (Carbonation Test, Netterburg, 1984).

(vi) Place erosion specimen in measuring jig (see Photo Plate A.9 use specimen number on tray as a reference point for subsequent measurements) and take the measurements at the preselected positions on the jig, using a Vernier caliper. Record all data on erosion test sheet (see Figure A.2).

A.4.6.4 Preparation of erosion test device

(i) Place three erosion specimens in erosion test device, again using the specimen number as a reference point to ensure that specimens are always placed in the same relative positions in the erosion test device.

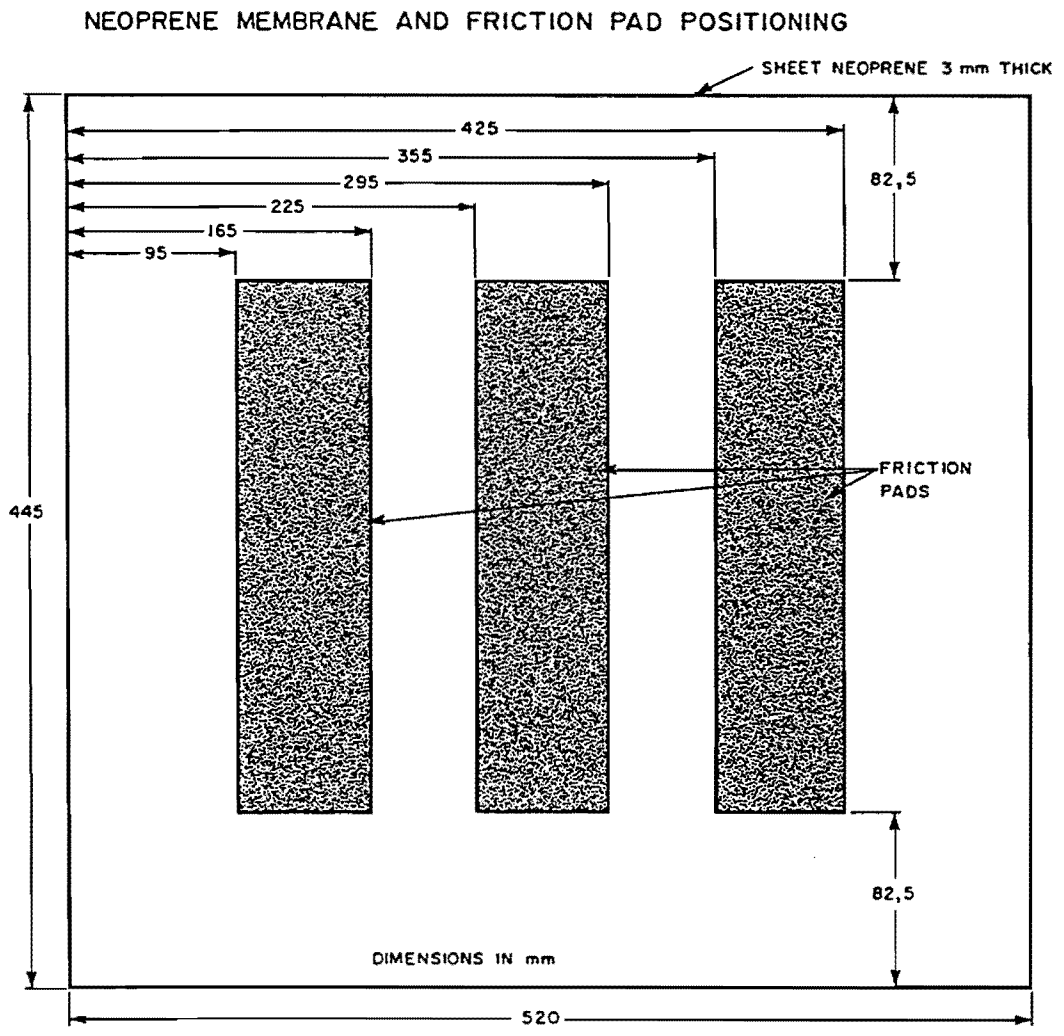

Figure A.2 Neoprene Membrane and Friction Pad Position.

NOTE: If specimens are cut to less than 75 mm, spacers under the specimens tray must be introduced so as to maintain a total height of approximately 75 mm.

(ii) Tighten specimen tray retaining clamps.

(iii) Position neoprene rubber membrane and ensure that it is always used in the same relative position for the duration of the test. (Ensure that friction pads are on the underside of the membrane). See also Photo Plate A.5.

(iv) Position retaining frame over the membrane and clamp at the four corners.

(v) Fill the test tray with water until it overflows at the elevated vents. Maintain a head of water by means of a tube connected to the water tap and placed in one of the vents.

(vi) Lower the three tracking (loading) wheels on to the membrane, set the counter at zero and start the erosion test device.

(vii) At the required number of erosion repetitions (counter x 2) remove the erosion specimens and repeat from Section A.4.6.3 (iii) to (vi) without the need for soaking, leaving loose aggregate (> 4.75 mm) on the surface of the specimen.

NOTE : The required number of erosion repetitions to determine the erosion index, L, is 5000. The erosion index, L, is defined as the average depth of erosion after 5000 erosion load repetitions in the erosion test device, measured from 15 positions on the erosion specimen, using the measuring jig and Vernier caliper. For research purposes, the depth of erosion may be determined, if needed, after every 500 repetitions in order to obtain the rate of erosion in mm per erosion repetition.

A.5 PRODUCTION OF FRICTION PADS

This section, describes the production of the friction pad used in the erosion test device. The necessary apparatus for this production are listed in Section A.2.9.
In this case the production of 30 friction pads is described, but the quantities listed can easily be adjusted for the production of different quantities of friction pads.

(i) Number ten sheets of Norton P80 Tuffback wet or dry abrasive paper (Item A.2.9.1 in Section A.2.9) from 1 to 10 and record the mass of each sheet.

(ii) Place piece of scrap paper in clipboard and clamp a sheet of abrasive paper by its very edge with the abrasive surface uppermost.

(iii) Pour entire 500 ml of pliobond into a plastic bag and tie up the open end with a rubber band to completely seal the bag. Invert the bag and cut off one corner to make a small aperture. Stand in a suitable container to keep upright and prevent leaking.

(iv) Fill the 400 ml beaker with acetone (approximately 200 ml) and stand the brush therein.

(v) Place clipboard on a balance, note mass, and from the plastic bag squeeze approximately 23 grams of pliobond on to the abrasive paper. Using the paintbrush, quickly spread evenly over the entire surface and replace in beaker with acetone.

(vi) Without delay, dump an excess of Crystolon crystals (Item A.2.9.2) on to the prepared surface, and using the specimen tray (Item A.2.6.1), firmly bed the grit on to the prepared surface.

(vii) Remove the scrap paper, together with the abrasive paper and excess grit, and place to one side. Repeat the process, making a total of four. The first one should now be dry enough to recover the excess of grit by tipping it on its side. This excess (loose) grit is added to the supply to be used in making further pads. When number five is made, recover grit from number two, etc. On completion of the ten pads, they are left for 24 hours to cure at 21°C.

(viii) Each pad is now firmly rubbed with the palm of the hand to dislodge any loose particles. A distinct difference between a loose or firm surface can be felt. Shake the pad to remove the loose grit and record the mass of the coated pad.

(ix) Subtract the uncoated mass from the coated mass to establish the mass of the grit retained. Should this be greater than 145 g, rub the coated surface with a rubber pad to reduce the grit mass to 145 g, if possible.

(x) Place 30 ml pliobond and 30 ml acetone into the 80 ml beaker and dilute the pliobond. Use the paintbrush for mixing. Pour 50 ml of the mixture on to the pad and with the paintbrush distribute the mixture to evenly cover the surface. Should it be necessary, use part of or all of the remaining 100 ml mix. Place the pad aside and make a new mix in the same proportions, e.g. if only 50 ml was used, fill to 35 ml mark with pliobond and to 60 ml mark with acetone, i.e. 25 ml pliobond and 25 ml acetone added to the 10 ml remainder. After treating all ten pads, cure them in the sun for two hours and then in an oven at 70°C for one hour.

(xi) Mark off the pads in 70 mm widths across the 230 mm width of pad and score heavily from the underside with the steel rule and Stanley knife. The individual widths can now be pulled apart to form three pads of 70 mm x 280 mm. The mass of each pad should be 55 g, plus or minus 5 g (50 g - 60 g).

A.6 CALCULATIONS

A.6.1 Determination of the wet mass required for a target relatively modified AASHTO density

(i) List of symbols :

MDD = Maximum dry density of stabilized material (modified AASHTO compaction)

OMC = Optimum moisture content of stabilized material (TMH1 method A14)

C = Percentage stabilizer required according to TMH1 method A14 or based on experience, durability requirements or economical factors.

V = Volume of specimen = 450 mm x 75 mm x 75 mm

M1 = Mass of dry raw material

M2 = Mass of dry raw material plus excess dry raw material

M3 = Mass of dry raw material (M2), plus mass of stabilizer total

M4 = Mass of total wet mix

100k = Percentage relative density

M5 = Mass of wet mix required at k density

(ii) Formulae :

M1 = (MDD*V)/(1+C/100) A.1

M2 = M1 + 200 (Excess of 200 g dry raw material) A.2

M3 = M2 + (C/(100*M2)) A.3

M4 = M3 (1 + OMC/100) A.4

M5 = k [(MDD * (100 + OMC) * V)/100] A.5

A.6.2 Example calculation

Calculate the mass of materials required for an erosion specimen comprising soil and 4 percent cement, where

MDD = 2025 kg/m3

OMC = 9.2 percent

C = 4 percent

k = 95/100 (95 percent Mod. AASHTO required density)

(i) Mass of dry raw material, in situ compaction : 95 percent Mod. AASHTO, M1

= (MDD * V)/(1 + c/100)

= [2025 * 0.450 x $(0.075)^2$]/(1 + 4/100)

= 4929 g

(ii) Add 200 g for excess :

M2 = M1 + 200

$= 4929 + 200$

$= 5129$ g

(iii) Add mass of 4 g cement :

$M3 = M2 (1 + C/100)$

$= 5129 (1.04)$

$= 5334$ g

(iv) Add mass of OMC :

$M4 = M3 (1 + OMC/100)$

$= 5334 (1 + 9.2/100)$

$= 5824$ g

(v) Mass of wet mix required :

$M5 = k [(MDD * (100 + OMC) * V)/100]$

$= 0.95 [(2025 * (100 + 9.2/100) * 0.450 * (0.75)^2)/100]$

Therefore $M5 = 5317$ g

In order to obtain an erosion specimen at a target density of 95 percent of modified AASHTO and 4 percent cement, 6317 g of wet mix (soil, cement, and water) must be compacted in a beam specimen of the dimension 450 mm x 75 mm x 75 mm, using dynamic or static or both methods of compaction.

Figure A.3. Photo Plates of The Erosion Test Device and Accessories.

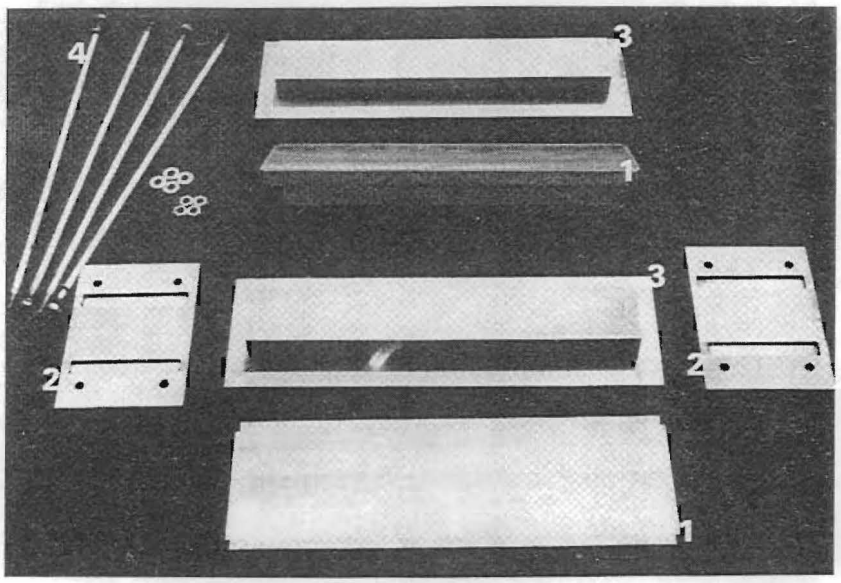

(a) Layout of the compaction mould: two side plates (1); two end plates (2); top and bottom plate (3); high tensile steel rods (4)

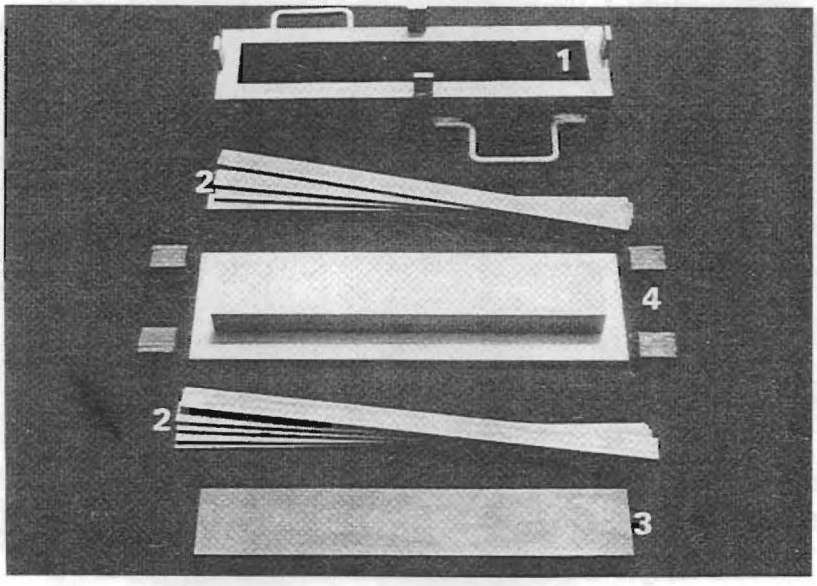

(b) Layout of the extention (1); metal space bars (2); phenol resin base plate (3) and rubber blocks (4) to be used in conjunction with the compaction mould in (a).

PLATE A1: COMPACTION MOULD AND ACCESSORIES.

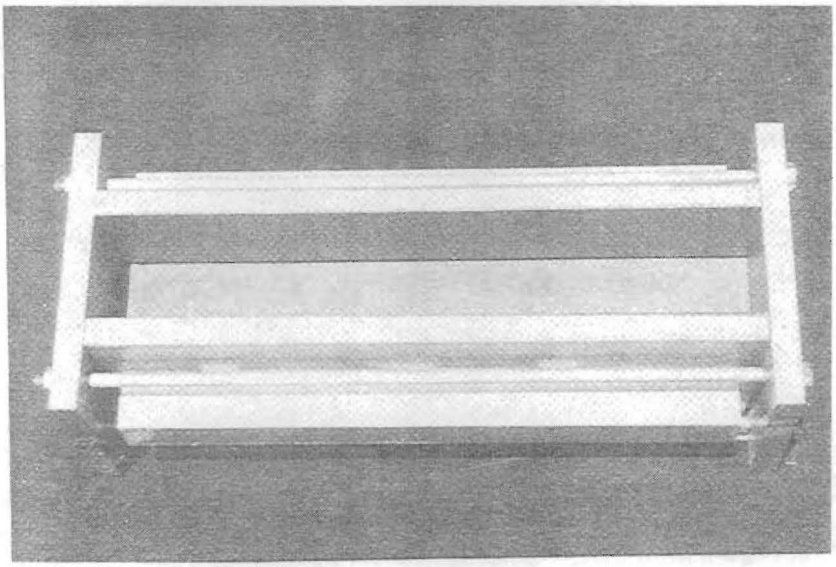

(a) Compaction mould with base plate in position.

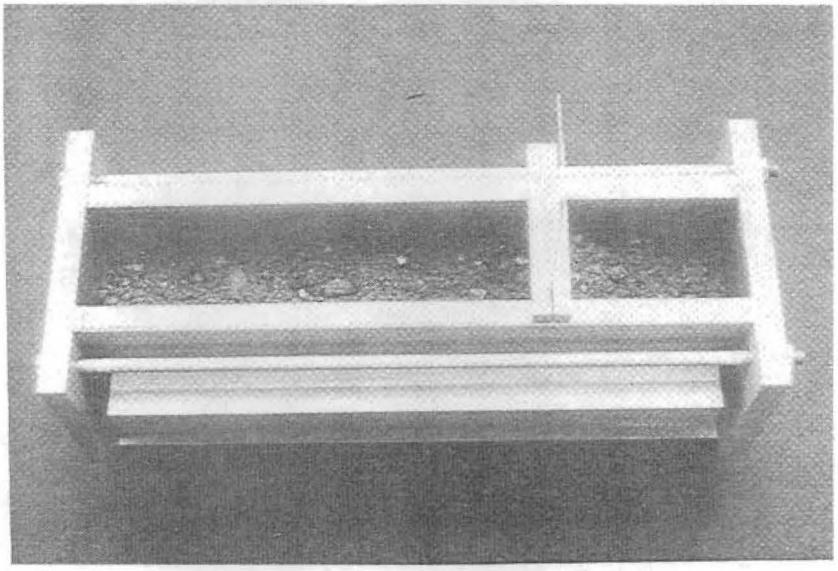

(b) Compaction mould with loose cementitious soil and spatula.

PLATE A2: ASSEMBLED COMPACTION MOULD.

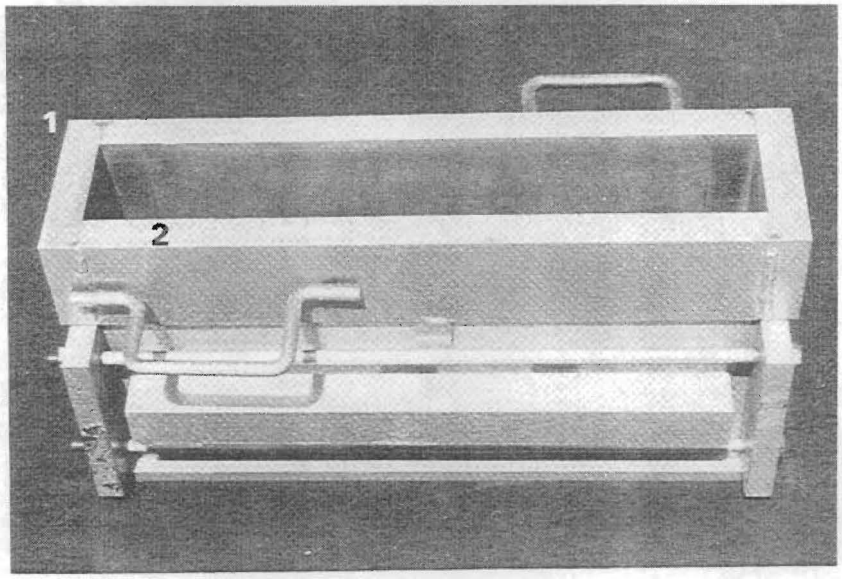

(a) Compaction Mould with extention (1) needed for dynamic compaction at predetermined positions for compaction hammer, (2) on the extention.

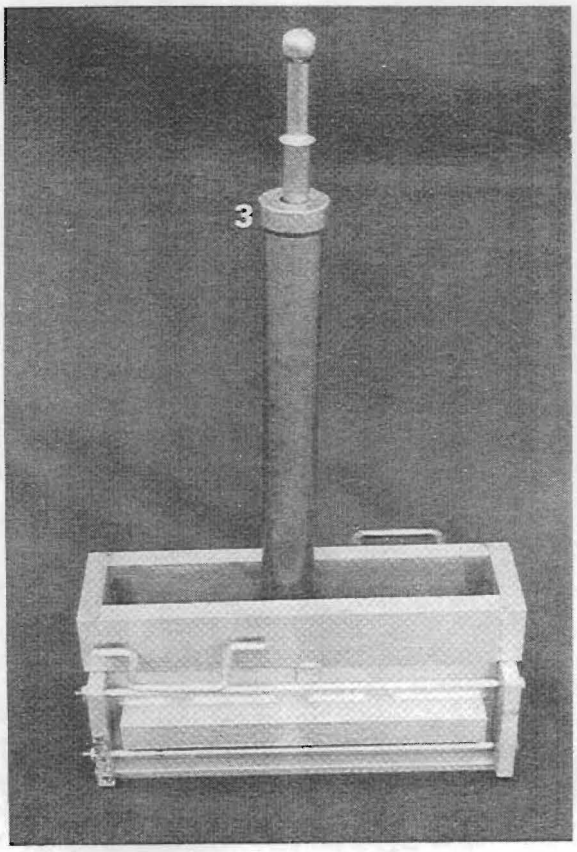

(b) Dynamic compaction using a Modified AASHTO hammer (3).

PLATE A3: COMPACTION MOULD WITH EXTENTION AND MODIFIED AASHTO HAMMER.

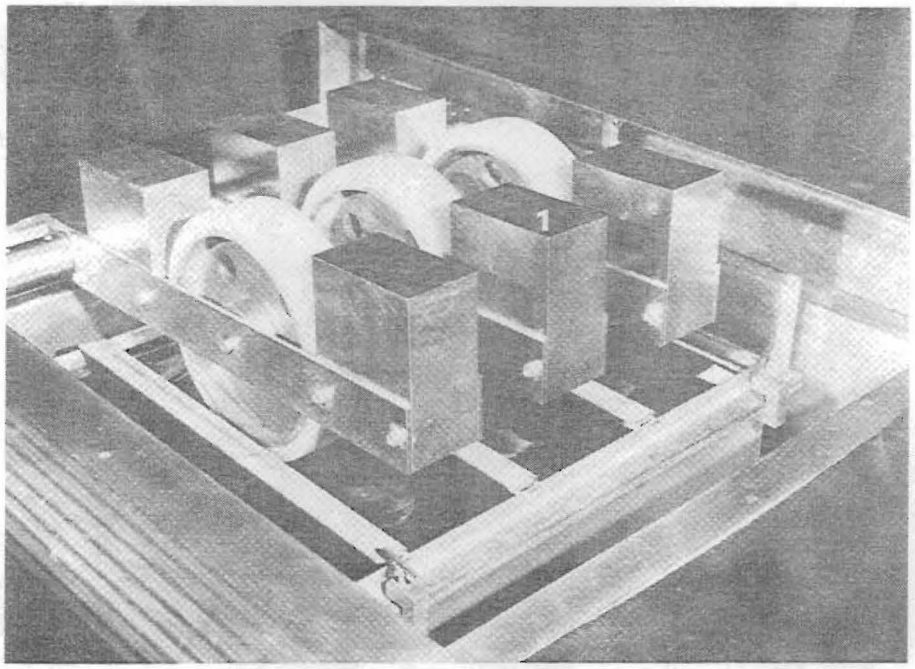

(a) Erosion Test device – with the three lineary driven loaded wheels (1) in position.

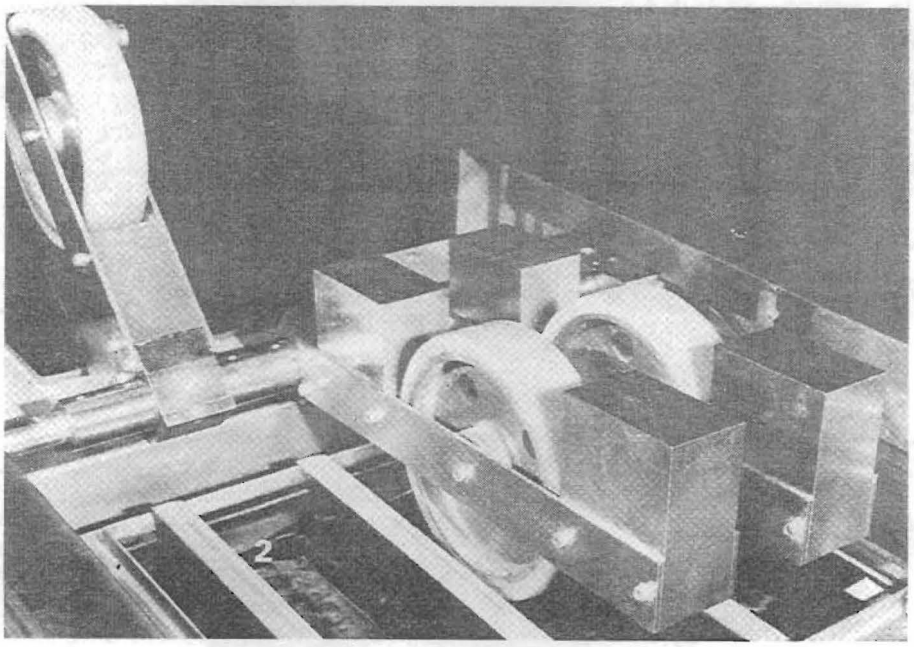

(b) Erosion Test device. Note the black neoprene flexible membrane (2) under the wheels.

PLATE A4: EROSION TEST DEVICE.

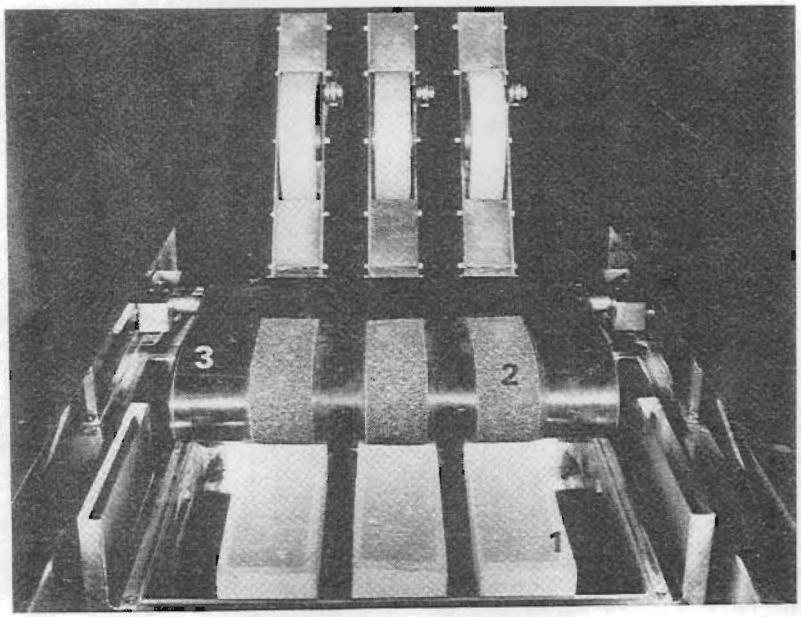

(a) Erosion Test device with three prepared specimens (1) in test position. Note also the friction pads (2) glued onto the black flexible neoprene membrane (3).

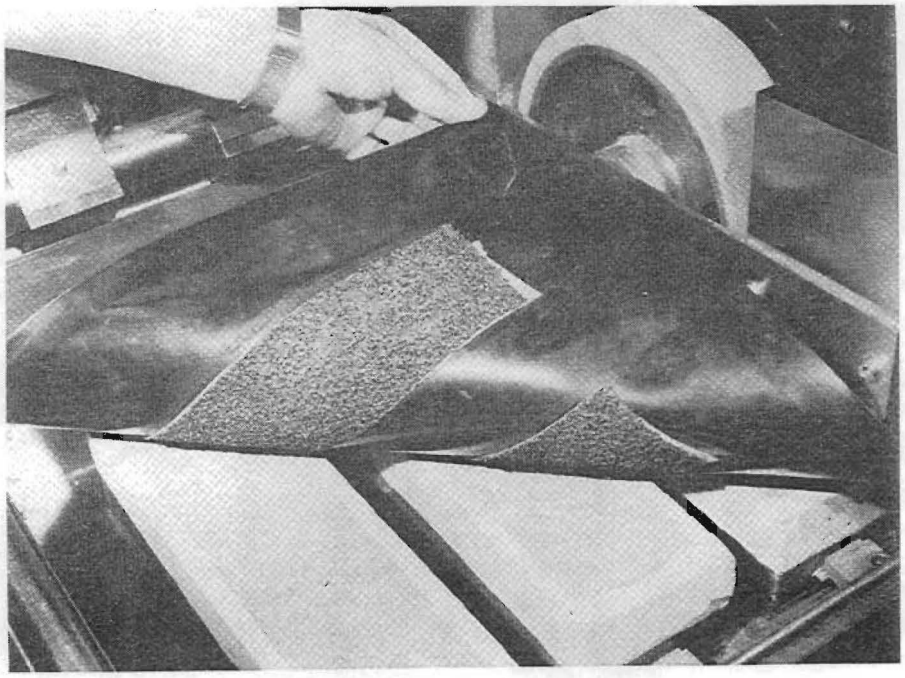

(b) Close view of the friction pads. (Two wheels are in the unload position.)

PLATE A5: FRICTION PAD WITHIN THE EROSION TEST DEVICE.

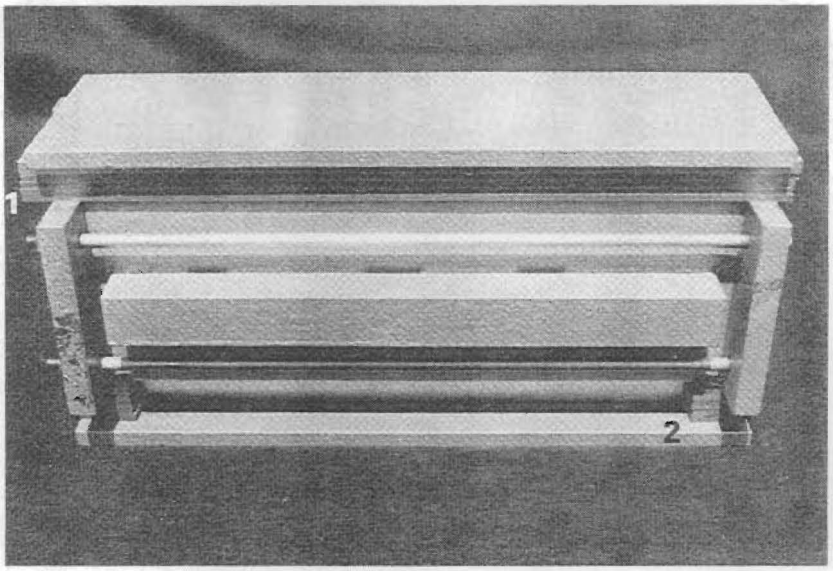

(a) Compaction mould with metal bars (1) and rubber blocks (2) used during static compaction.

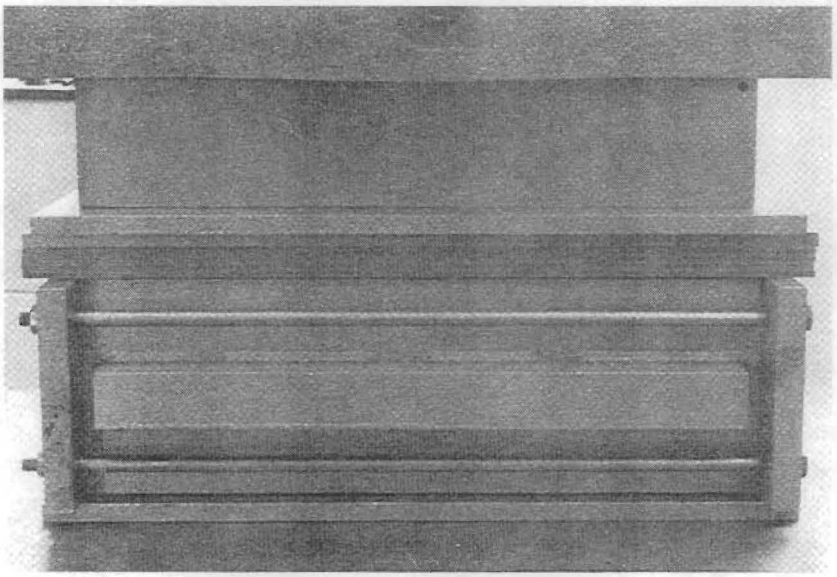

(b) Setup for static compaction in loading facility.

PLATE A6: STATIC COMPACTION OF EROSION BEAM SPECIMEN.

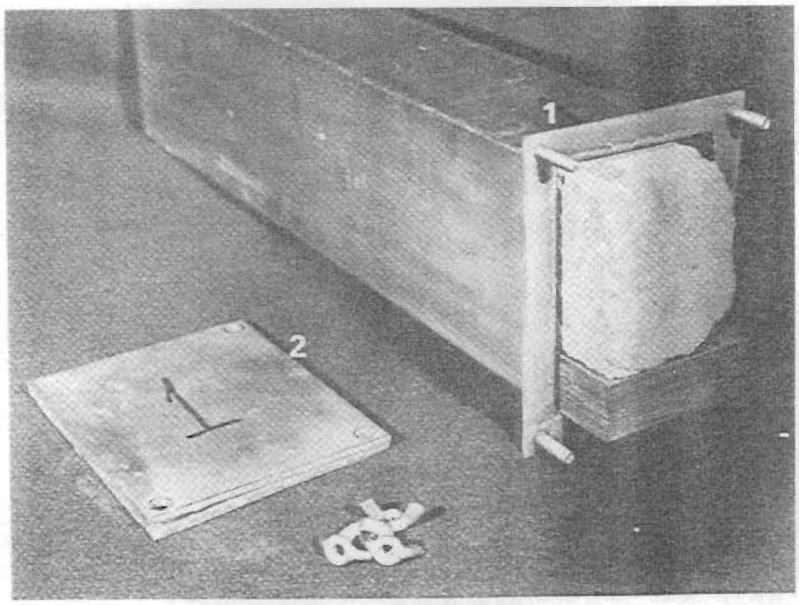

(a) Curing chamber (1) with air tight seal cap (2).

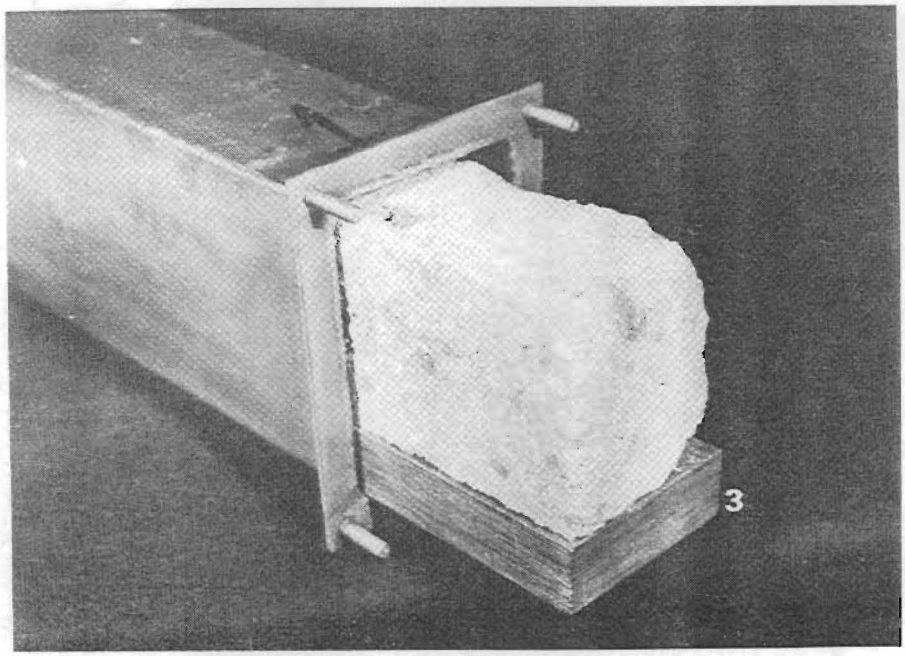

(b) Specimen on fabric based phenol resin base plate (3) in the curing chamber.

PLATE A7: CURING CHAMBER FOR CURING OF THE EROSION SPECIMEN.

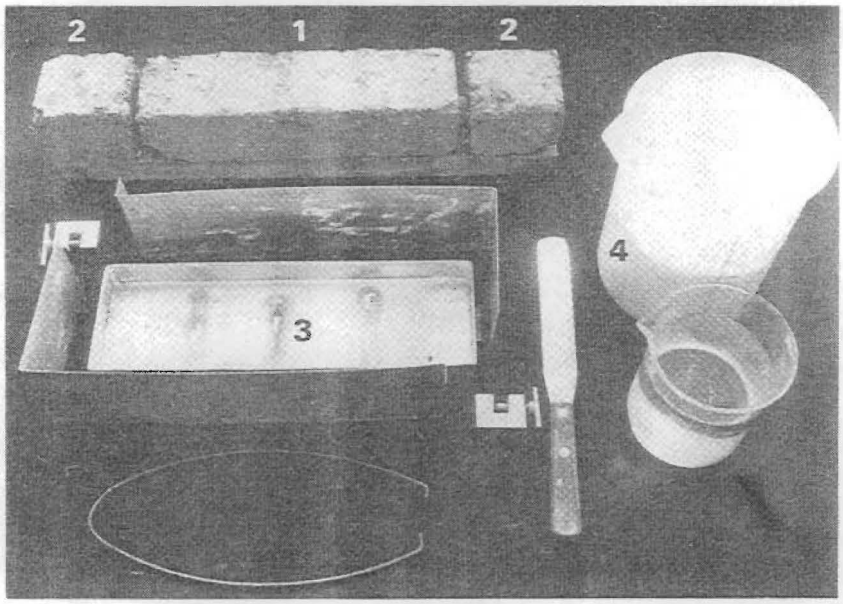

(a) Erosion specimen (1); two UCS specimens (2) and the apparatus for moulding the specimen with gypsum (3).

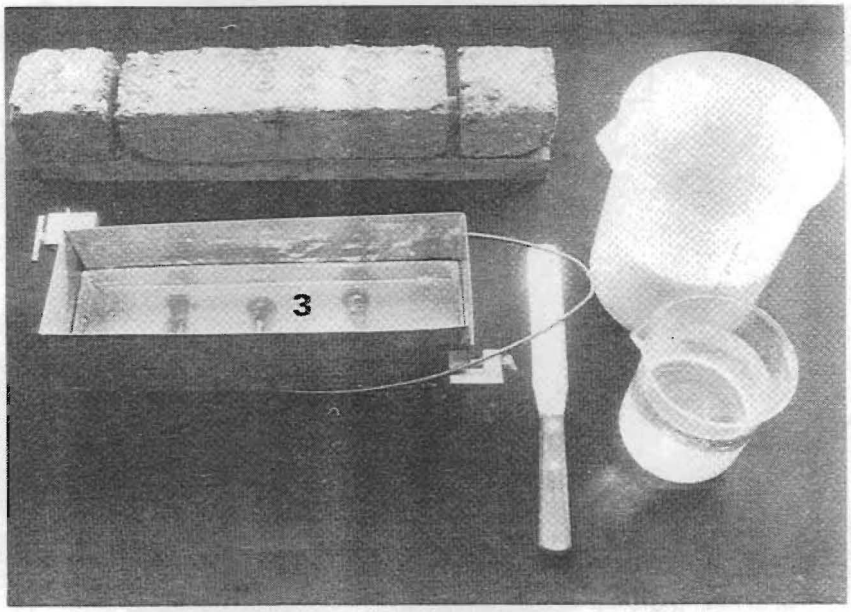

(b) Assembled moulding apparatus (3).

PLATE A8: MOULDING OF EROSION SPECIMEN WITH GYPSUM.

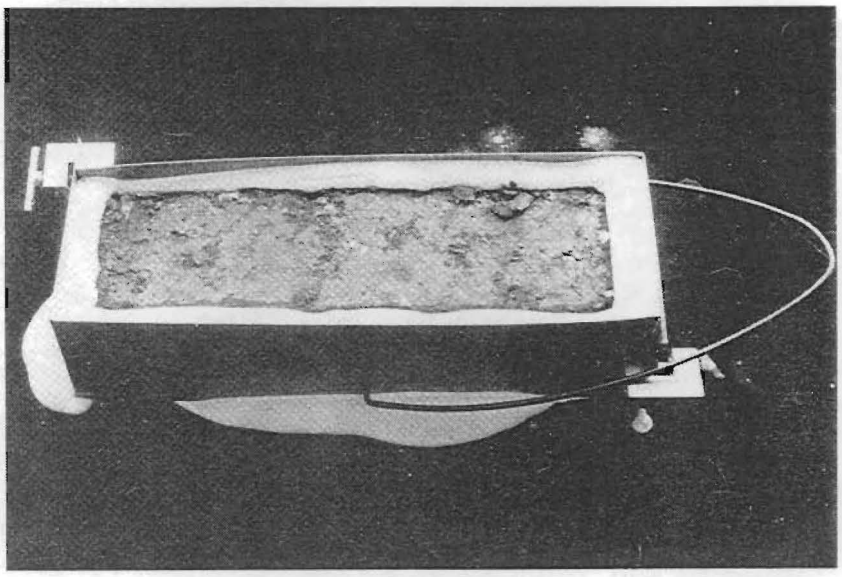

(a) Moulded erosion specimen.

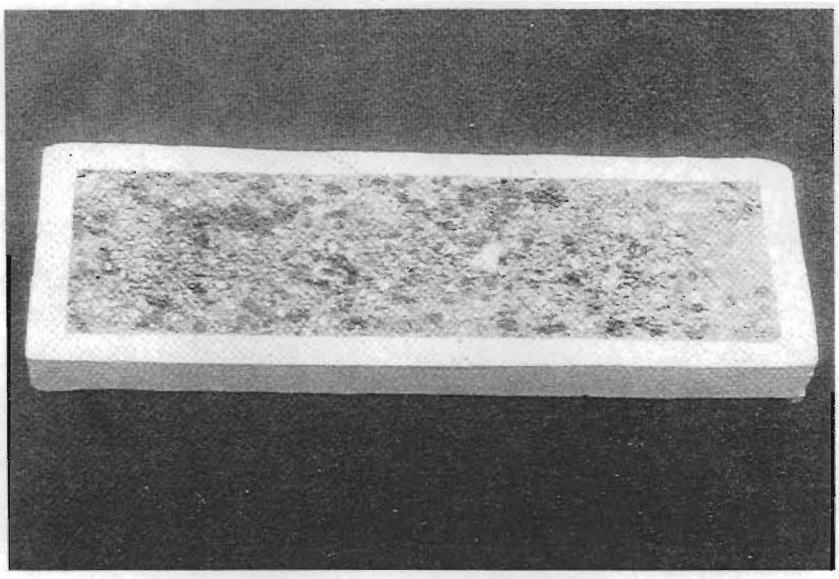

(b) Saw cut prepared erosion specimen ready for erosion testing.

PLATE A9: MOULDED AND SAW CUT PREPARED EROSION SPECIMEN.

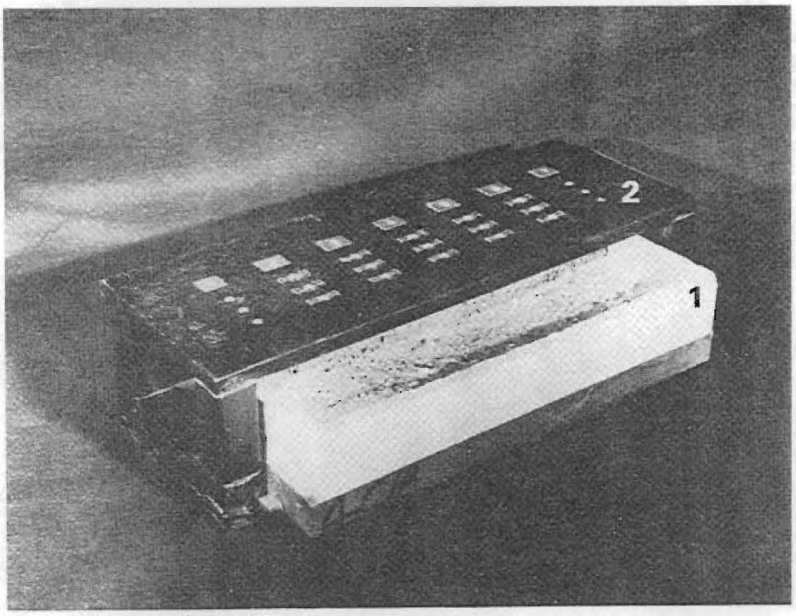

(a) Erosion specimen (1) in the meauring jig (2) in order to measure the depth of erosion on the surface of the specimen.

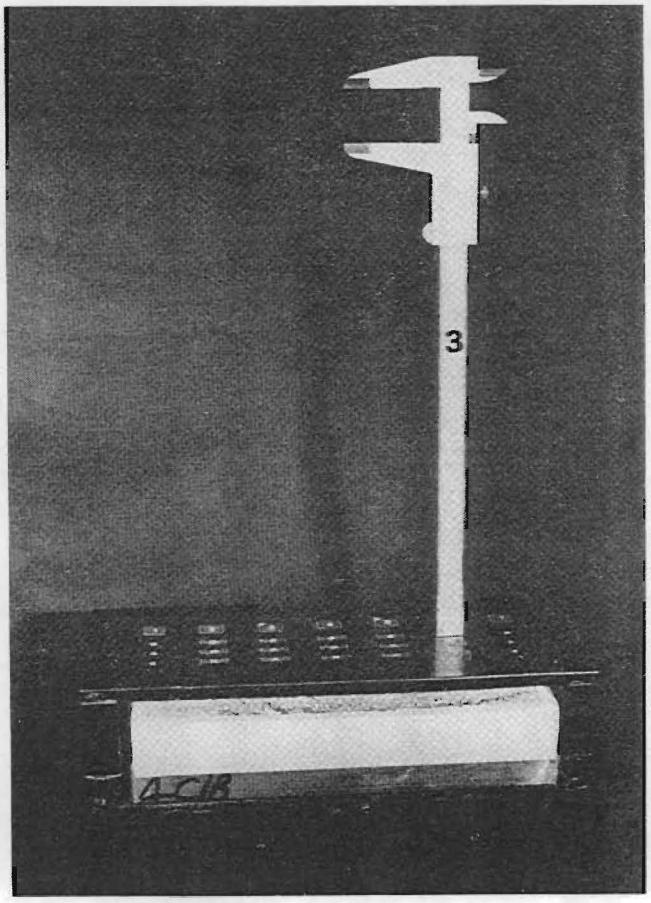

(b) Vernier caliper (3) for measuring the depth of erosion on the fifteen (15) fixed positions on the erosion specimen.

PLATE A10: MEASUREMENT OF THE DEPTH OF EROSION.

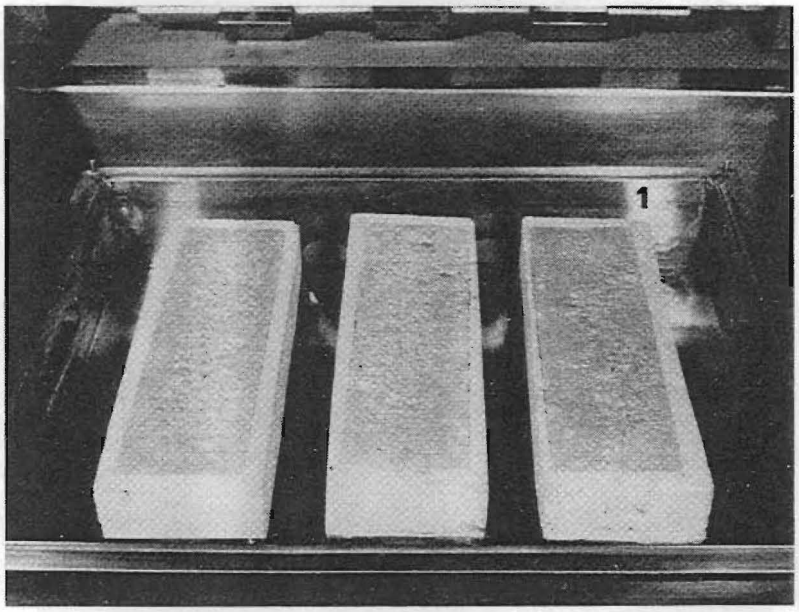

(a) Three erosion specimens in position in the water bath (1) (without water) of the Erosion Test device, before testing.

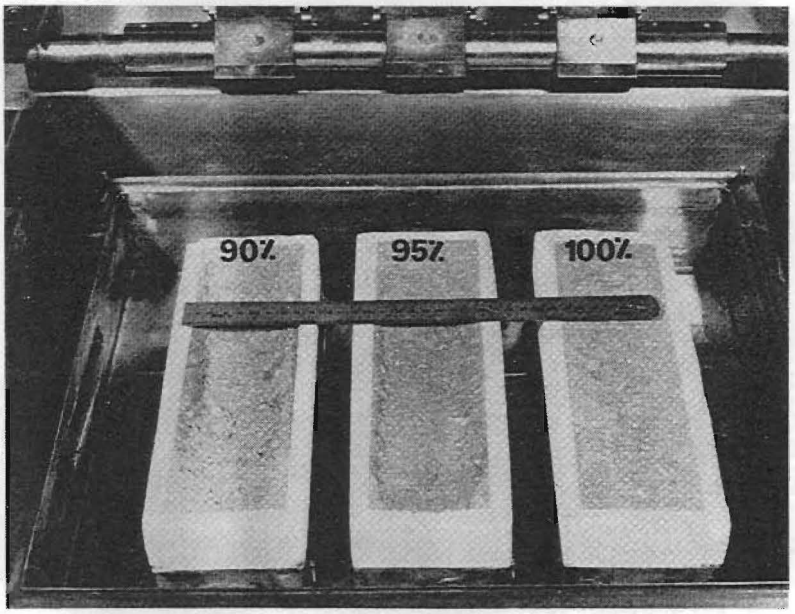

(b) Three erosion specimens after testing. The three specimens were compacted at different relative modified AASHTO compaction densities ie 90%, 95% and 100%. Note the difference in depth of erosion on the surface of these specimens.

PLATE A11: EROSION TEST SPECIMENS IN EROSION TEST DEVICE BEFORE AND AFTER TESTING.